Communications Research Centre

PROPAGATION MEASUREMENTS FOR LAND-MOBILE SATELLITE SERVICES IN THE 800 MHz BAND

by

J.S. Butterworth
Mobile Studies Group
Directorate of Space Systems

Government of Canada
Department of Communications

Gouvernement du Canada
Ministère des Communications

CRC TECHNICAL NOTE NO. 724

OTTAWA, AUGUST 1984

Canada

COMMUNICATIONS RESEARCH CENTRE

DEPARTMENT OF COMMUNICATIONS
CANADA

PROPAGATION MEASUREMENTS FOR LAND-MOBILE SATELLITE SERVICES IN THE 800 MHz BAND

by

J.S. Butterworth

Mobile Studies Group
Directorate of Space Systems

CRC TECHNICAL NOTE NO. 724

August 1984
OTTAWA

Table of Contents

Table of Contents (con't)

PROPAGATION MEASUREMENTS FOR LAND-MOBILE SATELLITE SERVICES IN THE 800 MHz BAND

by

J.S. Butterworth

ABSTRACT

A measurement program was undertaken with the objective of providing engineering design data on excess path-loss for a land-mobile satellite system operating in the 800 MHz band. In the suburban and rural areas which could be served by such a satellite system, multipath fading and shadowing by terrain obstacles were the main phenomena to be characterized. In the absence of a suitable satellite source, various simulation methods were used. Measurements of deciduous foliage attenuation gave a value of 0.29 dB per metre of foliage depth. At a source elevation angle of 15 to 20 degrees the mean signal attenuation in shadowed locations was 7 dB, with less than 10.4 dB at 95% of the locations in the test area. Measurements of fading statistics in unshadowed locations, using a conical log-spiral antenna, showed the diffuse multipath signals to be typically 11 dB below the direct component. Measurements of the combined effects of fading and shadowing over 50 km of rural roads showed that excess-loss margins above minimum quality of about 14 dB would be required to provide service to 99% of the locations at 20° elevation angle. At 15° a margin of about 20 dB would be required.

1. INTRODUCTION

1.1 SUBJECT

In considering the implementation of a land-mobile satellite system, one of the more important decisions to be made is the choice of a suitable excess path-loss margin for the link to the mobile users. An excessively high margin could make the system too expensive to be viable by requiring a very high output power from the spacecraft. On the other hand, too low a margin could result in unsatisfactory service due to the frequent occurrence of signal dropouts. The measurement program described in this report was considered necessary as very little objective information was available on which to base the choice of margin. In fact the only information published was on work by Hess, sponsored by NASA, describing

measurements made using the ATS-6 satellite (Hess, 1980). Hess made his measurements using a vertically-polarized whip antenna on the mobile; most of the areas characterized were urban centres. The results showed that satellite coverage of urban areas was not feasible in either the 800 MHz or 1500 MHz band due to the heavy shadowing effects of tall buildings. However, the advantage of a satellite system is in being able to provide coverage in areas outside cities where the low user density will not support the cost of a terrestrial base-station network. The objective of the Communications Research Centre measurement program, initiated in the Spring of 1981, was to provide engineering design data on excess path-loss for a satellite system providing suburban and rural coverage.

1.2 PURPOSE AND SCOPE

The purpose of this report is to present a description of the measurement methods used to characterize the path-loss statistics of a simulated satellite source as received at a mobile and to present and discuss the results obtained. At the start of the program, we decided to conduct the measurements using an electrically representative mobile antenna, i.e. circularly-polarized and with an optimized radiation pattern, rather than using a whip antenna.

As the ATS-6 satellite used by Hess was no longer functioning and there were no other operational satellites with a high-output capability in this frequency band, we simulated a satellite source in various ways. Reception at the mobile was favoured over transmission as this was more convenient operationally. Additional measurements made using an L-Band satellite source for land mobile applications are the subject of a separate report (Butterworth, 1984).

1.3 PLAN OF DEVELOPMENT

To enable a build-up in expertise and sophistication of measurement techniques, the program was conducted in three phases:

- static measurements of the attenuation caused by shadowing effects of roadside terrain features
- mobile measurements of received signal-strength of a signal source suspended from a tethered balloon
- mobile measurements of signal-strength from a source carried by a helicopter

This report is therefore divided into three main sections which describe the three phases of the measurement program in chronological order.

2. STATIC MEASUREMENTS

In the mainly rural areas served by a mobile communications satellite, the most frequent shadowing obstacles are likely to be roadside

trees. For this reason, the objective of the first phase of the program was to characterize the attenuating effects of foliage. The measurements were performed for elevation angles in the range of 15 to 24 degrees.

2.1 FACTORS INFLUENCING EXPERIMENTAL PROCEDURES

In making measurements of foliage attenuation, the objective is to measure the absorption effect to the exclusion of multipath and diffraction effects. This can be achieved by locating the receiver in the deeply-shadowed zone where the diffracted wave is much less than the transmitted wave (Lee, 1982 Sec. 4.2). Multipath effects, which cause a standing-wave field of maxima and minima, can be averaged out by making multiple measurements with the receive antenna moved a half-wavelength or so between measurements. This spatial separation is sufficient to de-correlate the measurements (Lee, 1982, Sec. 9.4). The absorption effect can be quantified by taking a similar set of readings in a nearby location which is not shadowed, avoiding the need for absolute calibration.

2.2 DESCRIPTION OF PROCEDURES

To provide a source at a sufficient altitude, a circularly-polarized antenna was mounted on the top of a 64m tower (a part of the David Florida Lab antenna range). The antenna was designed and mounted in such a way as to illuminate the surrounding terrain at a suitable distance from the tower. A signal generator powered the antenna, via a coaxial cable, from a hut at the base of the tower.

Seven measurement sites, shadowed mainly by deciduous trees, were chosen at various points around the tower. Figure 1 shows the general disposition of the equipment. Four nearby comparison sites were chosen with clear line-of-sight to the top of the tower. The antenna used to receive the signal was a circularly-polarized conical log-spiral. Figure 2 shows construction details of this antenna. The radiation pattern was omnidirectional in azimuth with the elevation pattern shaped to provide as much gain as practical in the region of 15 - 30°. Figure 3 shows the measured elevation plane pattern. In use, the antenna was placed on top of a field intensity meter, which was used as the receiver. The meter in turn was supported on a wooden box, so that the base of the antenna was about 0.6m above ground level.

Measurements were taken twice weekly at all sites from April 28th to November 4th, 1981, spanning the time from when the leaf buds were starting to open until after the leaves had fallen. For reasons explained previously, at each site the average value of five readings was recorded, with the equipment being moved about half a wavelength (17 cm) between readings. The foliage depth was estimated at each site and an average value calculated. This was to enable a final result to be presented in terms of dB/m of foliage depth in addition to an overall figure.

2.3 PRESENTATION OF DATA

Figure 4 shows a plot of the smoothed cumulative percentile curve of a set of individual readings (i.e. without averaging) on a Gaussian probability scale. The fact that these results, expressed in dB of attenuation, fall close to a straight line, indicates that the underlying distribution is log-normal. This provides the rationale for averaging readings in decibels rather than converting to linear units, as may otherwise be required to obtain an accurate estimate of mean values.

For each day on which measurements were taken, five readings were made at each of the seven sites. These were then averaged to obtain a single attenuation figure for the mean foliage depth of 24 metres. Figure 5 shows a time plot of the readings obtained. The solid regression line is a fourth-order polynomial fit to the data. The order of fit was selected on the basis of minimizing the standard error of estimate (the standard deviation of the data points about the line). The dashed lines are spaced from the regression line by an amount equal to twice the standard error of estimate (i.e. 2 X 1.7 dB). 95% of the data points would be expected to fall between these limits. The graph shows an increase in attenuation as the leaves develop in the spring, a relatively constant attenuation in summer and a decrease as the leaves dry out and fall in the autumn. A summary of the main statistics during the summer period is:

Probability distribution: log-normal
Mean value (in full leaf): 7 dB
Standard error of estimate: 1.7 dB
95 percentile attenuation: 10.4 dB
Mean foliage depth: 24m
Mean attenuation/metre depth: 0.29 dB/m

2.4 INTERPRETATION OF DATA

The result of 0.29 dB/m obtained compares favourably with a projection of 0.3 dB/m made by extrapolating measurement results at frequencies up to 600 MHz (Rice, 1971, Fig. 1). CCIR Report 236-5 suggests values in the range 0.2 to 0.3 dB/m, depending on foliage density and ambient conditions. These independent sources give added confidence to the result. A further conclusion is that a mobile passing close to a shadowing deciduous woodland area could typically experience a mean signal attenuation of 7 dB, with a loss of no more than 10.4 dB for 95% of the locations, for elevation angles in the range 15 to 24 degrees. These figures are exclusive of the additional losses due to multipath effects.

3. MOBILE MEASUREMENTS WITH A STATIONARY SOURCE

The foliage attenuation program was of limited scope because of the inefficiency of taking readings manually and the fact that measurements could only be made at a limited number of specific sites. To expand the scope of the program, shortly after the start of the foliage attenuation program, arrangements were made to borrow a mobile laboratory and to equip

it to take readings automatically at certain increments of distance travelled. In this way, thousands of digitized readings could be stored in a few minutes, permitting characterization of both fading and shadowing effects for a larger cross-section of terrain types.

To provide a source at a suitable altitude, we used tethered weather balloons to carry aloft a small transmitter and antenna. This provided a suitable signal source which could be set up in a few minutes at almost any location.

3.1 FACTORS INFLUENCING EXPERIMENTAL PROCEDURES

Obviously in using a tethered balloon at a limited height, the distance which could be driven by the mobile before a significant change of range or elevation angle occurred was very limited. Usually the distance was increased by locating the tether point near a bend in a road, such that if the bend was considered to be part of a sector of a circle, the tether point was at its centre. However, the variety of terrain which could be included in each data set was quite limited.

In making mobile measurements, the effects of Doppler shift of the direct signal and Doppler spreading of the multipath signals must be considered when choosing appropriate receiver IF and video bandwidths. These factors are also appropriate to Section 4 of this report where use of a mobile source is discussed.

3.1.1 REQUIRED RECEIVER IF BANDWIDTHS

In communications with a mobile vehicle, the characteristics of the received signal are influenced by the motion of both the vehicle and, in the general case, of the source. For example, a satellite source with no north-south stationkeeping (such as MARECS A) can reach a range-rate from some areas of almost 40 km/h twice in its daily cycle, with a concurrent small change in look-angle.

The mobile, illuminated by the source, moves along in a standing-wave field caused by the summation of the direct signal and its various components scattered towards the mobile by the surrounding terrain. The received direct component is Doppler-shifted with respect to the source frequency by an amount:

$$f_d = (\pm RR \pm V \cos\Theta \cos\alpha)/\lambda$$

where:

RR = source range-rate
V = mobile speed
Θ = source elevation angle
α = angle of vehicle heading from source azimuth
λ = source wavelength

The choice of plus or minus is governed by relative vehicle and source motion components. For vehicles moving at freeway speeds, f_d can be as high as 100 Hz.

If the vehicle is traversing a uniformly-scattering plane, the received scattered components will arrive uniformly from all directions and will have Doppler shifts and energy spectral densities depending on their angle of arrival relative to the vehicle heading. The maximum Doppler shift will be $f_m = \pm V/\lambda$, by scattering from terrain directly ahead of or behind the vehicle. The energy spectral density will be (Clarke, 1968, Eq. 27):

$$S(f) = \frac{1}{f_m \sqrt{1 - f^2/f_m^2}}$$

where f is the received frequency difference from the centre frequency $f_c = f_s \pm RR/\lambda$ (f_s is the source frequency). Outside the range $f = \pm f_m$, the energy spectral density is zero. Figure 6 shows the shape of the RF spectrum. The receiver IF bandwidth therefore needs to be at least 2 f_m in order to pass the full Doppler spectrum.

3.1.2 REQUIRED VIDEO BANDWIDTH AND SAMPLING RATE

The spectrum of the linearly envelope-detected baseband signal extends in frequency to 2 f_m and may include two peaks, depending on vehicle heading relative to the source azimuth (Clarke, 1968, Fig. 7b). Figure 7 shows a typical case. In order to sample, digitize and store the baseband output, the sampling rate should be at least 4 f_m and preferably higher to avoid sampling errors. In spatial terms, this is equivalent to at least four samples per wavelength travelled. In practice samples were taken every 5 cm, which is equivalent to about seven samples per wavelength.

3.2 DESCRIPTION OF PROCEDURES

Figure 8 shows the equipment used in the mobile laboratory. The signal received by the conical log-spiral antenna was amplified and envelope-detected by the field-strength meter, set to its narrowest IF bandwidth of 10 kHz. The high-speed digital voltmeter digitized the demodulated output of the field-strength meter each time a trigger pulse was received from the odometer take-off. The digitized readings were stored on magnetic tape by the desktop computer, coupled to the voltmeter by a general-purpose interface bus (GPIB). Recording speed was limited by the unsatisfactory video bandwidth of the field-strength meter, which was only 10 Hz. This limited driving speed to 6 km/h, because of the considerations outlined in para. 3.1.2.

An inverted conical log-spiral antenna, similar to the one shown in Fig. 2, housed the transmitter electronics and batteries. The electronics (Fig. 9) consisted of a 210 MHz crystal oscillator, followed by two frequency-doublers and a 28 dB gain amplifier, powered by two 6-volt lantern batteries. The EIRP was of the order of a few milliwatts. The total

package weight of about 2 kg was suspended from a meteorological balloon inflated with about four cubic metres of helium. The balloon was usually tethered at about 300m altitude in a location which would result in an elevation angle of 15 to 20° from the measurement site. The measurements were made at a variety of sites to establish typical ranges of statistical parameters under both line-of-sight and shadowed conditions.

3.3 PRESENTATION OF DATA

Data recorded under line-of-sight conditions in completely open terrain were modelled quite accurately by the Rice distribution, described by Norton (Norton, 1955). Fig. 10 shows a comparison between a typical data set and a Rice distribution. Most data sets recorded were of size 1000 - 5000 points. Other data sets, taken at different sites, resulted in the following Rice parameters (multipath/constant component ratio) for best fit to the data:

File No:	Rice Parameter (K): (dB)	Elevation Angle: (degrees)
MC31	-10	7
MC32	-14	14
MC33	-12	18
MC41	-10	14
MC42	-10	13

The parameter K = 20 log (root-sum-square of the random component amplitudes divided by the constant component amplitude). Data sets were also recorded at sites shadowed by various types and densities of tree foliage. Figure 11 shows several examples of the results obtained, plotted relative to the unfaded, unshadowed signal level. This level was estimated by calculating the median value of a thousand readings of received level taken at a nearby unshadowed location. As noted in the first phase of the program, shadowing effects tend to follow a log-normal distribution. For this symmetrical distribution, the mean and the median are equal and the standard deviation can be obtained as the dB difference between the 84% and the median value of the distribution function.

3.4 INTERPRETATION OF DATA

For completely open terrain, the diffuse multipath components scattered towards the receiving antenna by the surrounding terrain (grassland and the roadbed) were found to be in the region of 10 - 14 dB below the direct signal, with an average of about 11 dB. The Rice distribution modelled the data closely. For shadowed sites, foliage and multipath losses caused mean attenuations as high as 9 dB, with standard deviation of 6 dB, depending on foliage density. The log-normal distribution modelled variations of the data.

Although these results gave an idea of the range of the statistical parameters, they were not very useful as engineering design data,

as they were based on very small samples of terrain. For this reason, the next phase of the program was designed in such a way as to enable the characterization of about 50 km of rural roads.

4. MOBILE MEASUREMENTS WITH A MOBILE SOURCE

During the previous phase of the program, the design and outfitting of a new mobile laboratory were undertaken to provide a continuously available facility. The vehicle chosen was a converted "minibus" of a size representative of the smaller commercial vehicle. In addition to being equipped to record digitized readings of signal strength without any limitation on driving speed, the new equipment also included an instrumentation tape-recorder to make "stored channel" recordings of the amplitude and phase variations of the signal. The purpose of this new inclusion was to enable subsequent laboratory simulation of the mobile communications channel by replaying the recordings and using them as control signals for a quadrature modulator.

The transmitter package was similar to the one used in conjunction with the meteorological balloons. In this case however, to simulate a far-distant satellite source, the transmitter was carried by a helicopter which kept pace with the mobile laboratory at a range of a few kilometers, such that a constant relative bearing was maintained.

4.1 FACTORS INFLUENCING EXPERIMENTAL PROCEDURES

The considerations outlined in Section 3.1 apply equally well to measurements using a mobile source. There is however, an assumption implicit in the method of making "stored-channel" recordings which should be explained here. It is that the signal bandwidth is less than the coherence bandwidth of the channel. In other words no frequency-selective fading effects occur within the signal bandwidth. Typically, the coherence bandwidth is at least 100 kHz so that the assumption is valid for all conditions of measurement. Under this narrow signal bandwidth assumption, the flat fading of the received signal, due to addition of the line-of-sight component and the multipath components scattered towards the receiver by the surrounding terrain, can be modelled as a multiplicative distortion of the type:

$$h(t) = I(t) + jQ(t)$$

Figure 12 shows the narrowband channel model. If the in-phase I(t) and quadrature Q(t) multiplying signals are independent Gaussian signals with zero mean, then Rayleigh fading results. If the mean value E(I) is not zero, then the presence of the constant component results in Rice fading.

The effects of shadowing by terrain obstacles (diffraction and absorption) also cause a variation in the values of I(t) and Q(t). As has been noted previously, the effects of these spatial factors can be modelled by the log-normal density function.

4.2 DESCRIPTION OF MOBILE LABORATORY

The mobile laboratory was designed for real-time recording of digitized samples of received signal-strength as well as for making tape-recordings of received signal amplitude and phase ("stored-channel" recordings). Figure 13 shows a block diagram of the equipment. A spectrum analyser was chosen as the receiver in place of the field intensity meter used previously. The advantages of the spectrum analyser were the ability to operate the instrument under computer control through the IEEE 488 GPIB, the wide range of IF and video bandwidths available, and a centre-frequency stability sufficient to allow measurements in 300 Hz bandwidth at frequencies up to 1600 MHz.

4.2.1 "STORED CHANNEL" RECORDING SYSTEM

The spectrum analyser, used in zero-scan mode during measurements, provided a 21.4 MHz IF output to a quadrature demodulator. The in-phase and quadrature outputs were recorded separately on two tracks of an instrumentation tape-recorder. This method of producing "stored channel" recordings was developed at DFVLR in Germany (Hagenauer, 1982). Other tracks of the same tape recorded a commentary channel, the demodulated output of the receiver and distance markers from the odometer.

4.2.2 DIGITIZED DATA RECORDING SYSTEM

The linearly envelope-demodulated output (video output) from the spectrum analyzer was also used as input to a chart recorder and to a high-speed three-and-a-half digit digital voltmeter. This voltmeter, used on its one-volt range, where its resolution was one millivolt, provided a 60 dB dynamic range in the digitized data. Used under control of a desktop computer, the apparatus was capable of digitizing and recording up to a thousand readings per second. Readings were triggered by pulses produced by the odometer subsystem, for every 5 cm travelled by the mobile laboratory. Readings were transferred from the voltmeter to the computer, via the GPIB, for storage on floppy discs. About 130,000 readings could be stored on each disc, corresponding to 6.5 km distance travelled by the vehicle. Trigger pulses were also supplied to the chart recorder to advance the paper in proportion to the distance travelled by the vehicle.

4.2.3 ANTENNA SYSTEM

The antenna used for most of the data collection was the same conical log-spiral used in earlier phases of the program. Before installation on the mobile laboratory, the antenna was overcoated with a layer of fibreglass to weatherproof it. This also changed the radiation pattern slightly, to that shown in Fig. 14 (measured without ground-plane). Fig. 15 shows the mounting arrangement for the antenna above the centreline of the vehicle roof. Fig. 16 shows an as-mounted antenna pattern obtained by making a mock-up of the vehicle roof, mounting the antenna on it and measuring the pattern in a large anechoic chamber.

4.2.4 ODOMETER AND POWER SUBSYSTEMS

The original odometer drive cable was disconnected from the dashboard instrument and a special gearbox was interposed between the two to give a second odometer drive output. This extra output rotated an optical-type shaft angle encoder providing 2500 pulses per revolution. By driving a measured distance it was ascertained that 1536 pulses were produced for each metre travelled by the vehicle. The pulse train was applied to a selectable-ratio divider. A division ratio of 77 resulted in one pulse for every 5.0 cm travelled by the vehicle.

The power subsystem consisted of two components. The first was an engine-driven high-output alternator with integral 12 volt regulator, capable of providing 100A at idle speed and 145A at full speed. The second component was a static inverter, used to convert the 12V input to 115V/ 60 Hz AC regulated output, with a maximum capability of 1000 VA. The installed equipment required about 700 VA.

4.3 DESCRIPTION OF TEST AREA

A test area was sought for the measurement program to satisfy the following criteria:

- convenient to both CRC and the aviation services contractor to minimize wasted travelling time.
- relatively flat terrain crossed by a series of straight parallel roads to enable relative road vehicle and helicopter positions to be maintained more accurately.
- terrain features to be sufficiently varied and yet well-characterized to enable both fading and shadowing effects to be studied.
- road orientation to be roughly perpendicular to the MARECS "A" satellite azimuth (121°) to provide for similar test conditions (i.e. source broadside to mobile laboratory) when performing future comparison tests using this 1542 MHz satellite source.

The area finally chosen was West Carleton Township, located just north west of Ottawa. Fig. 17 is a map of the area showing the particular routes used. Second-growth (immature) woodlands of mixed species constituted 35% of the land area, the rest being cleared land (40% was farm-land). One-third of the length of the test-routes ran through wooded areas. There were no significant built-up areas along the routes, which were of a total length of about 90 km. Roadside power-lines on wooden poles ran along most of the length of the routes. In some areas, the same poles also supported multi-conductor telephone cables. The ground was mostly medium-dry soil but included about 8% wetlands.

The four routes used were roadways of one lane for each direction and were categorized roughly as follows:

- a provincial highway with gravel shoulders and a good setback of roadside trees and powerlines.

- an unpaved (gravel) township road with no shoulders and very little setback of trees, etc.

- two paved regional (county) roads with gravel shoulders and reasonable setback.

4.4 DESCRIPTION OF PROCEDURES

At the beginning of each of the four test-routes, the helicopter hovered on-station at the planned altitude for a few minutes while various tasks were performed. Starting locations were chosen to provide clear line-of-sight between the two vehicles. Initially, walkie-talkies were used for communications but later a VHF radio supplied by the aviation services contractor was installed in the mobile lab. In both cases, intelligibility to the unaccustomed operator was low due to the very high background noise in the helicopter. During this starting period, the helicopter elevation angle was checked with a clinometer. When this was completed, the measurement run started by taking a data sample of 1000 readings of received signal strength on an unshadowed part of the test-route. This was done while both vehicle and helicopter were in forward motion. The median value of these readings provided an estimate of the unfaded, unshadowed signal level.

Once the line-of-sight level was established, the mobile lab. and the helicopter proceeded along their parallel routes at the same speed, maintaining a constant relative bearing. Digitized readings of received signal-strength were recorded in files of up to 130,000 readings (corresponding to distances of 6.5 km) on double-sided 13.3 cm diskettes of 260k bytes capacity. At the same time analog tape-recordings were made on half-inch tape of the I and Q outputs of the quadrature demodulator. Because of this latter requirement, the receiver (spectrum analyser) was used in linear mode rather than the more customary logarithmic mode so that the tape-recordings could be used directly as control signal sources for "stored-channel" simulation purposes. A more detailed description of the data acquisition methodology and software is given in Appendix 1.

4.5 PRESENTATION OF DATA

The individual data points were converted into dB levels relative to the average line-of-sight reference level for the particular route in question. The data were then grouped into class intervals of 1 dB in received signal strength and a relative-frequency histogram was computed. Next a frequency polygon was tabulated by conceptually joining the centre-points of the columns in each class-interval of the histogram. The frequency polygon was then integrated using the trapezoidal rule to obtain an ogive (cumulative percentile curve). The graphically-smoothed ogives were used to obtain an estimate of the distribution function of the relative received signal level. The level-crossing rate (LCR) was also calculated from the data and, using a method described by Lee (Lee, 1982, Sec. 2.8) the average fade duration was derived from a knowledge of the distribution function and the LCR. A more detailed description of the methodology and software used for data analysis is provided in Appendix 2.

The first measurement session was held in September 1982, while the deciduous trees were still in full leaf, using a chartered Hughes 300C helicopter. Although it was desirable to suspend the transmitter and antenna below the helicopter to ensure an even azimuth radiation pattern, this proved not to be practical and eventually the antenna was mounted on a frame attached to the right-hand side of the helicopter. Figure 18 shows the mounting arrangement. This doubtlessly resulted in an uneven pattern due to reflections from the helicopter and so increased the importance of the helicopter being always on the same heading during measurements. For the first session, an elevation angle of fifteen degrees was chosen, as this was the lowest service elevation angle which had been discussed and an initial evaluation of the worst-case seemed appropriate. Figure 19 shows the distribution function obtained by cumulation of the data from all four routes shown in Fig. 17. Because of gaps in coverage between files, the data represents a sample of size one million points or about 50 km distance. Fig. 20 shows the level-crossing rate while Fig. 21 shows the average fade duration.

In June of 1983 a second series of tests was held, this time with the aid of a Bell Enstrom helicopter. Measurements were made with the helicopter at various altitudes so as to provide elevation angles of 5, 15, 20 and 30 degrees. During the tests, the winds above 1000 m. altitude were quite strong and as a result, the pilot had some difficulty in holding the helicopter on the correct heading. This resulted in a great deal of variation from file-to-file in the data taken at 30^{o} elevation, giving a result which was not consistent with the data at lower elevation angles. Consequently, the 30^{o} data was reluctantly discarded. Figure 22 shows the distribution functions obtained at the lower elevation angles. Figure 23 shows the corresponding level-crossing rates and Fig. 24 the average fade durations.

During the recording of data at 5^{o} elevation angle, a slowly-varying fading of 7 - 8 dB fade depth was observed while traversing areas of open terrain. This was superimposed on the rapid variations due to diffuse multipath effects and is inferred to be due to specular reflection. The theoretical analysis presented in Appendix 3 gives strong support to this deduction.

4.6 INTERPRETATION OF DATA

The distribution functions (Figs. 19 and 22) can be divided into two areas. The part to the left of the "knee" has a Rician shape which seems to be insensitive to elevation angle. The part to the right, where the probability of the relative level in question being exceeded is greater, is of log-normal shape having an intercept point with the Rician part which varies with elevation angle. A full description of statistical modelling of the results shown in Fig. 19 has been given by Loo (Loo, 1984). The log-normal part of the distribution function is the part of interest for engineering design purposes, in that one is normally interested in designing a system to provide service to more than 90% of the locations.

As regards accuracy of the data, it is useful to compare the September 1982 data (Fig. 19) with the June 1983 data (Fig. 22) for 15^{o}

elevation angle. To provide coverage of 99% of the locations, for example, the earlier data indicates an excess-loss margin of 22.3 dB would be required. The later data indicates only 18.3 dB, a difference of 4 dB. In view of this difference and the variation in the individual files and line-of-sight reference level readings, it is estimated that the accuracy of the results in the log-normal region of the distribution function is about ±2 dB. It is probable that the main source of errors was the heading variation of the helicopter used for the June 1983 tests, coupled with the non-constant azimuth pattern of the transmitting antenna. Some files were unusable, whereas the data taken in September 1982 were all of good quality.

5. CONCLUSIONS

In the test area, deciduous foliage has an attenuation of 0.29 dB/m at 870 MHz during summer conditions. For a source at 15 to 20° elevation, the mean foliage attenuation in shadowed locations is 7 dB, with less than 10.4 dB at 95% of the locations. Signal statistics in shadowed locations are modelled by the log-normal distribution. Additional losses accrue due to multipath signal scattering towards the receive antenna. In unshadowed locations, the resulting fading due to summation with the direct signal can be modelled by the Rice distribution. In the test area, using the antenna described, the diffuse-to-constant component ratios of the best-fit Rician models to the data were in the range of -10 to -14 dB, with an average of -11 dB.

For a source at 15° elevation in the West Carleton region, the combined effects of fading and shadowing can result in a mean attenuation as high as 10 dB in certain areas. To provide service to, for example, 99% of the whole region, a margin of about 20 dB would be required at 15° elevation, or about 14 to 16 dB at 20° elevation. The accuracy of the analysed data is poorer than the test results obtained at 1540 MHz using a satellite source, due to various operational problems with the signal source. Excess-loss margin estimates for area coverage greater than 90% are likely to have an error of about ±2 dB.

At an elevation angle of five degrees, specular reflection in areas of open terrain caused slow fading with a depth of 7 to 8 dB to be superimposed on the rapid fading due to diffuse scattering.

6. ACKNOWLEDGEMENT

The results described in this report could not have been achieved without the dedicated and unstinting efforts of M. Dufour, E. Matt and R. Yank.

7. REFERENCES

1. Butterworth, J.S. 1984, "Propagation Measurements for Land-Mobile Satellite Systems at 1542 MHz", CRC Technical Note (in preparation).

2. Clarke, R.H. 1968, "A Statistical Theory of Mobile Radio Reception", The Bell System Technical Journal, Vol. 47, No. 6, July - August, pp. 957 - 1000.

3. Hagenauer, J. and Papke, W. 1982, "Data Transmission for Maritime and Land Mobiles using Stored-Channel Simulation", IEEE 32nd. Vehicular Technology Conference Record, pp. 379 - 383.

4. Hess, G.C. 1980, "Land-Mobile Satellite Excess Path-Loss Measurements", IEEE Trans. Vehicular Technology, Vol. VT-29, No. 2, pp. 290 - 297.

5. Lee, W.C.Y 1982, "Mobile Communications Engineering", New York, McGraw-Hill.

6. Loo, C. 1984, A Statistical Model for a Land-Mobile Satellite Link, IEEE International Conference on Communications, Conference Record.

7. Norton, K.A. et al. 1955, "The Probability Distribution of the Amplitude of a Constant Vector plus a Rayleigh-Distributed Vector", Proc. IRE, Vol. 43 No. 10, pp. 1354 - 1361.

8. Rice, P.L. 1971, "Some Effects of Buildings and Vegetation on VHF/UHF Propagation", IEEE Mountain West EMC Conference Record, pp. 1 - 10.

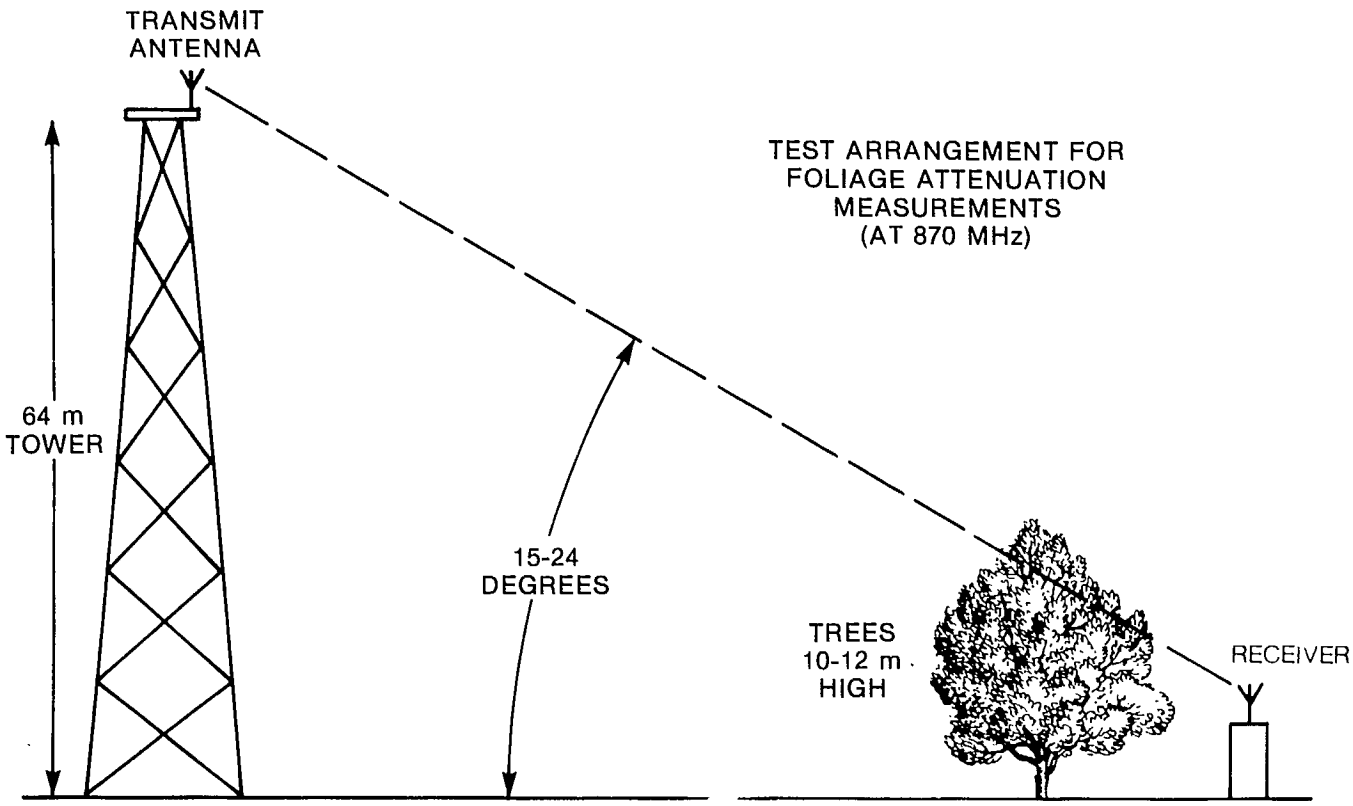

Fig. 1 Test arrangement for foliage attenuation measurements

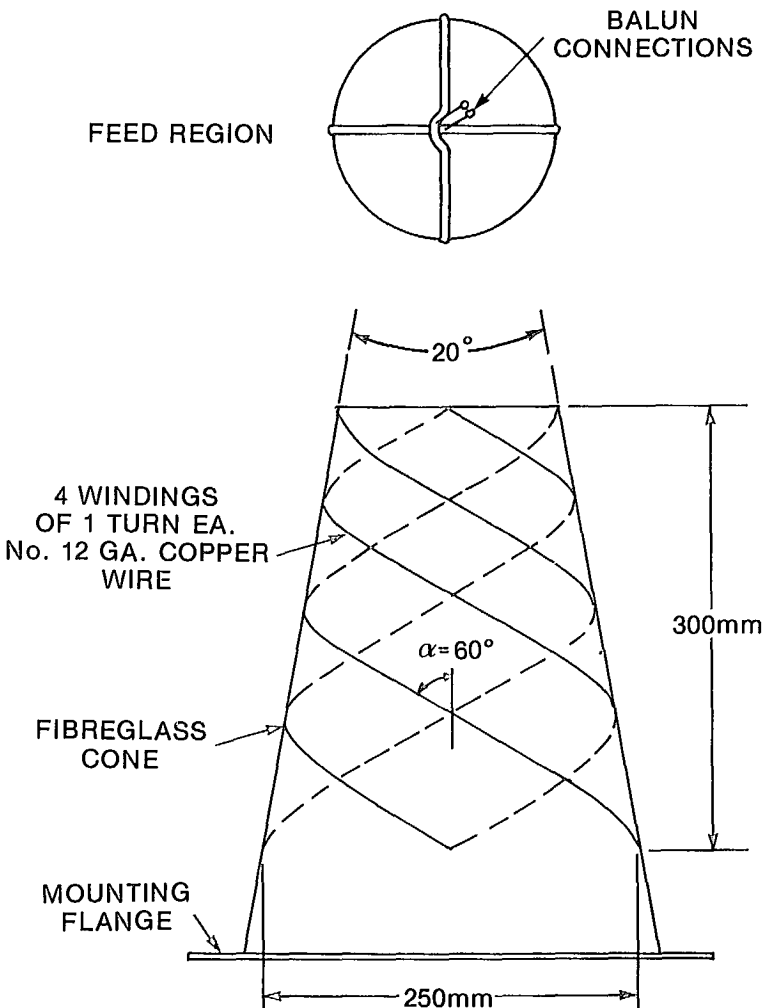

Fig. 2 Details of the conical-log-spiral antenna

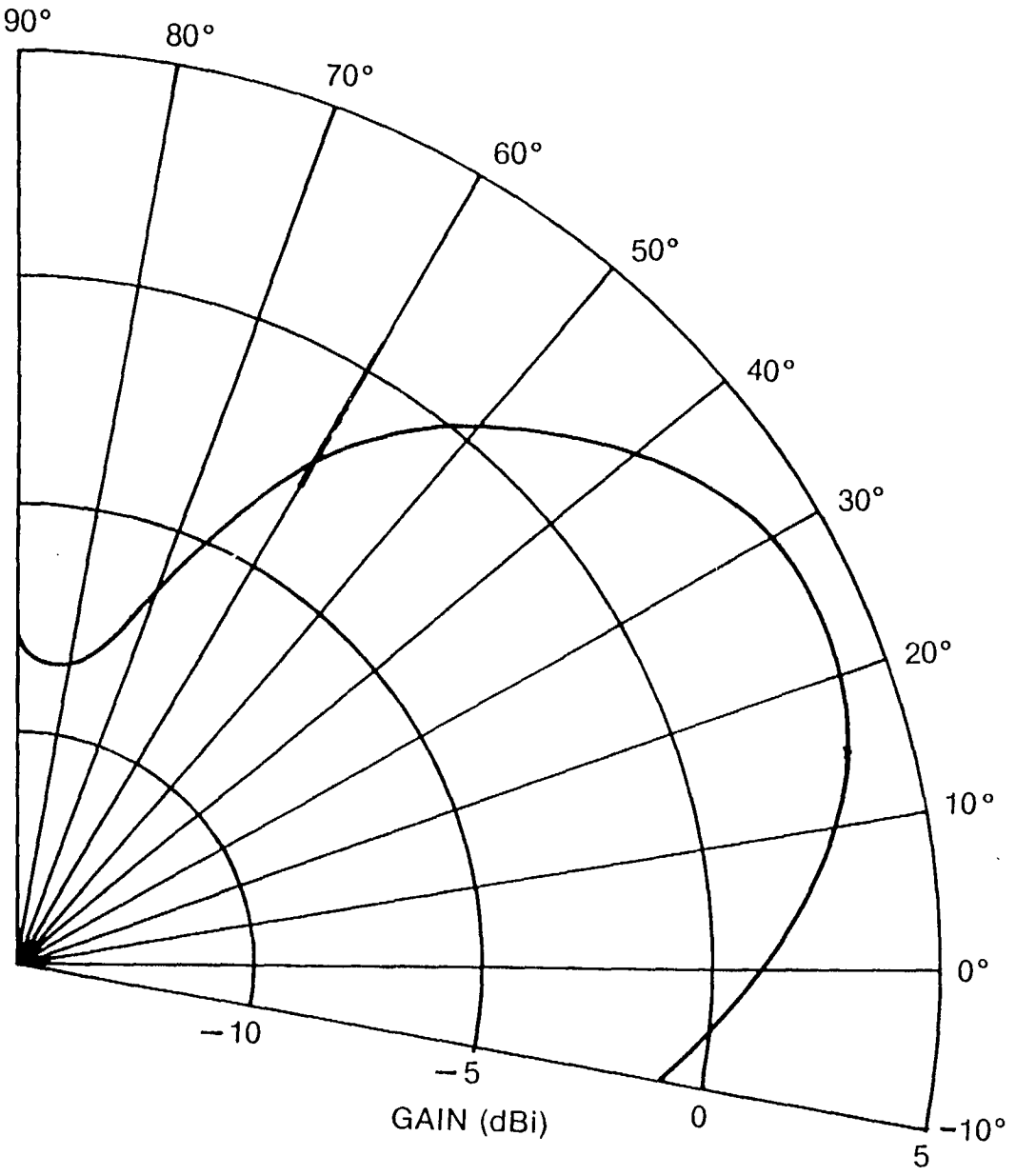

Fig. 3 Elevation-plane pattern of the conical-log-spiral antenna

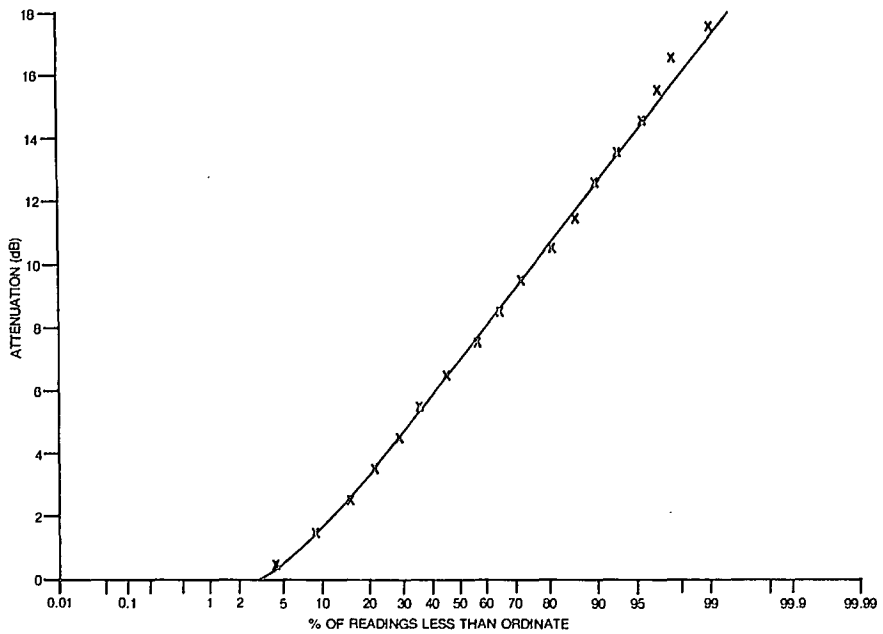

Fig. 4 Cumulative distribution of foliage attenuation readings for 1 - 19 June, 1981

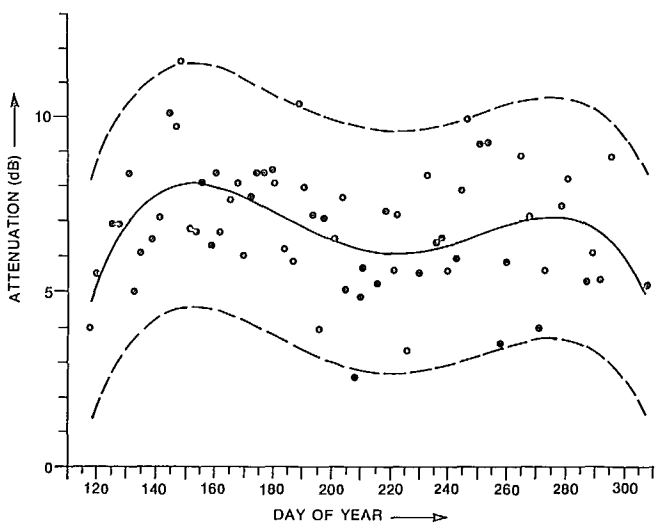

Fig. 5 Foliage attenuation data showing fitted curves

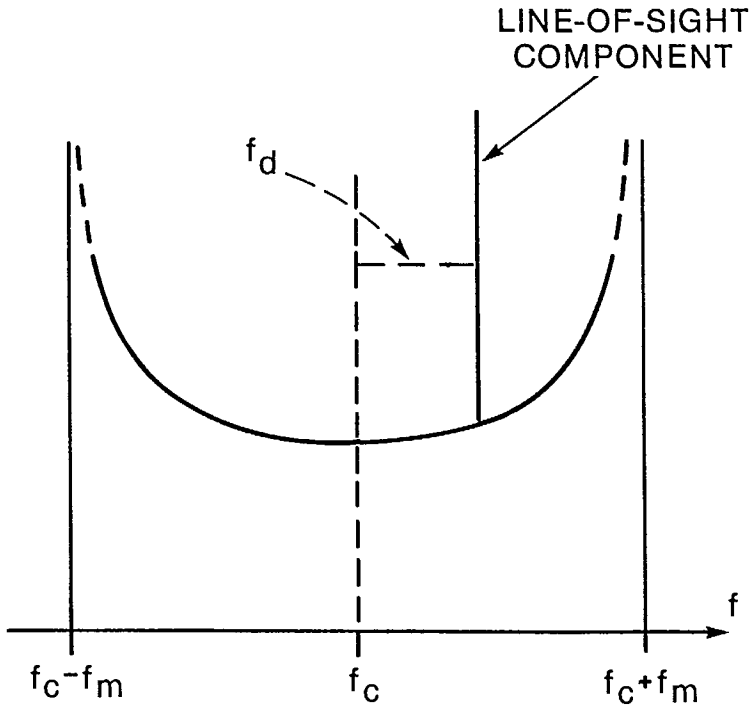

Fig. 6 Theoretical power spectrum of the multipath signals received by an omnidirectional antenna

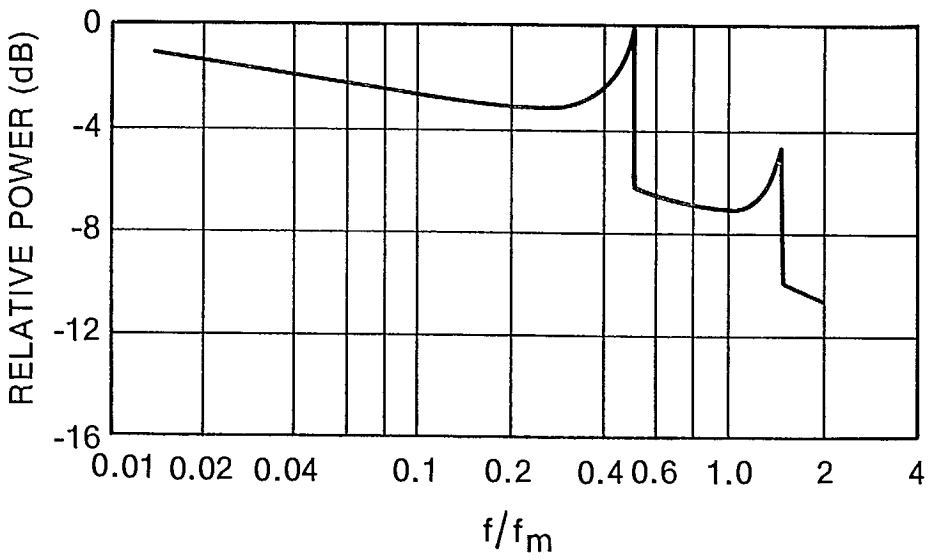

Fig. 7 Spectrum of the envelope-detected baseband signal corresponding to the RF spectrum of Fig. 6

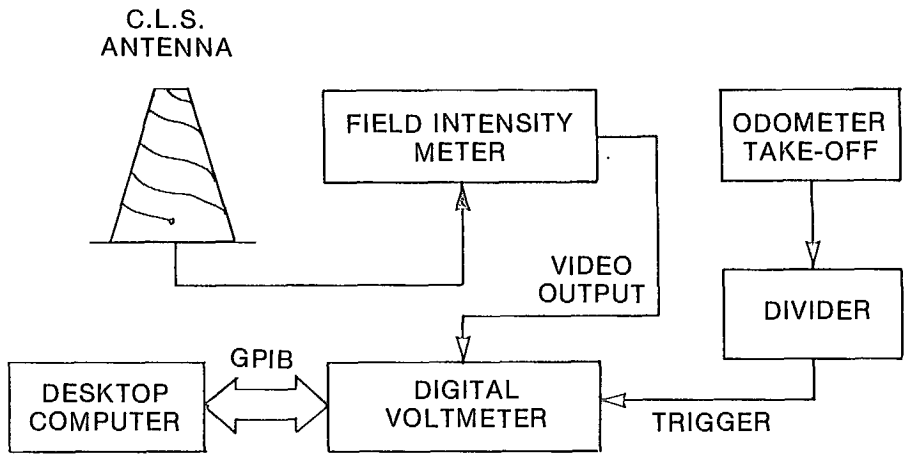

Fig. 8 Block diagram of the initial equipment used in the mobile laboratory

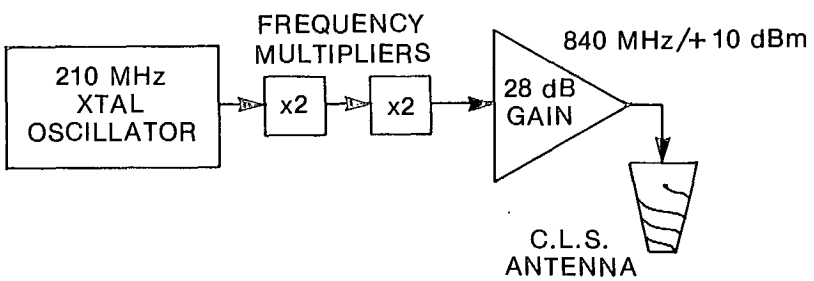

Fig. 9 Block diagram of the transmitter

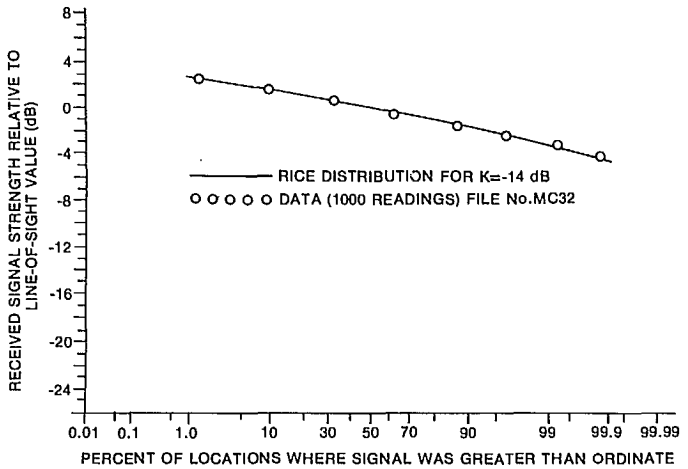

Fig. 10 Comparison of the distribution function of an unshadowed data set with a Rice distribution

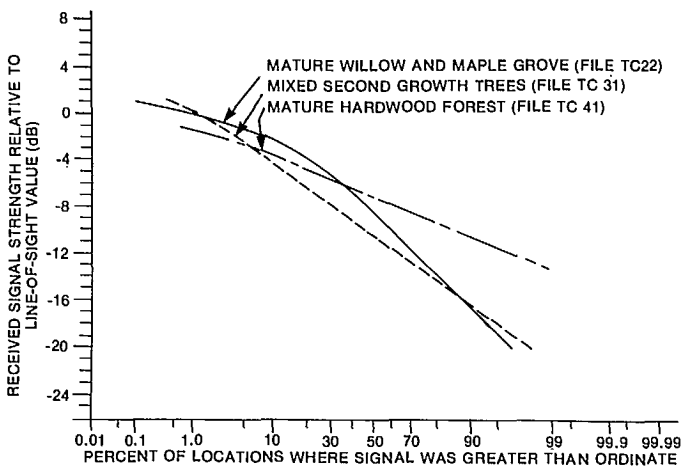

Fig. 11 Distribution functions of data recorded in various shadowed areas

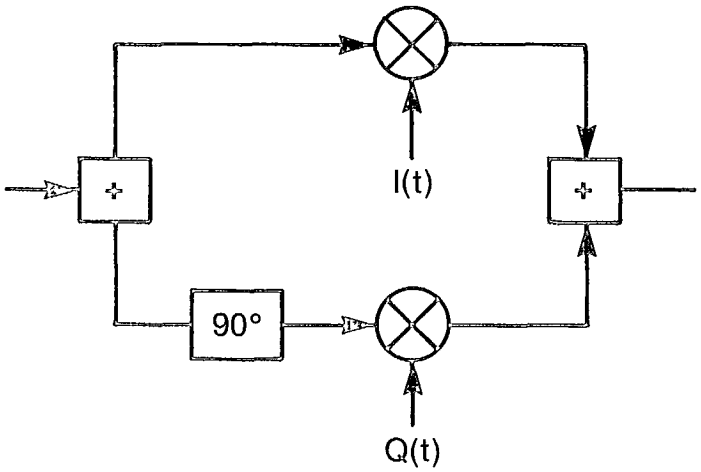

Fig. 12 Channel model and simulator

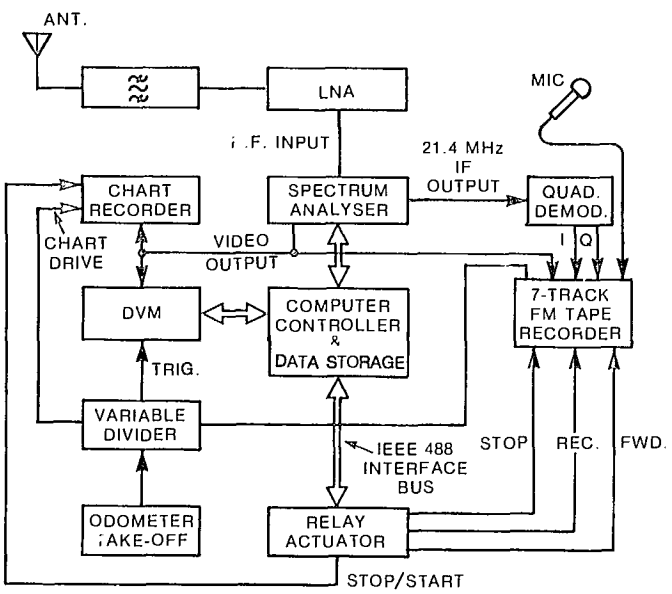

Fig. 13 Block diagram of the mobile laboratory equipment

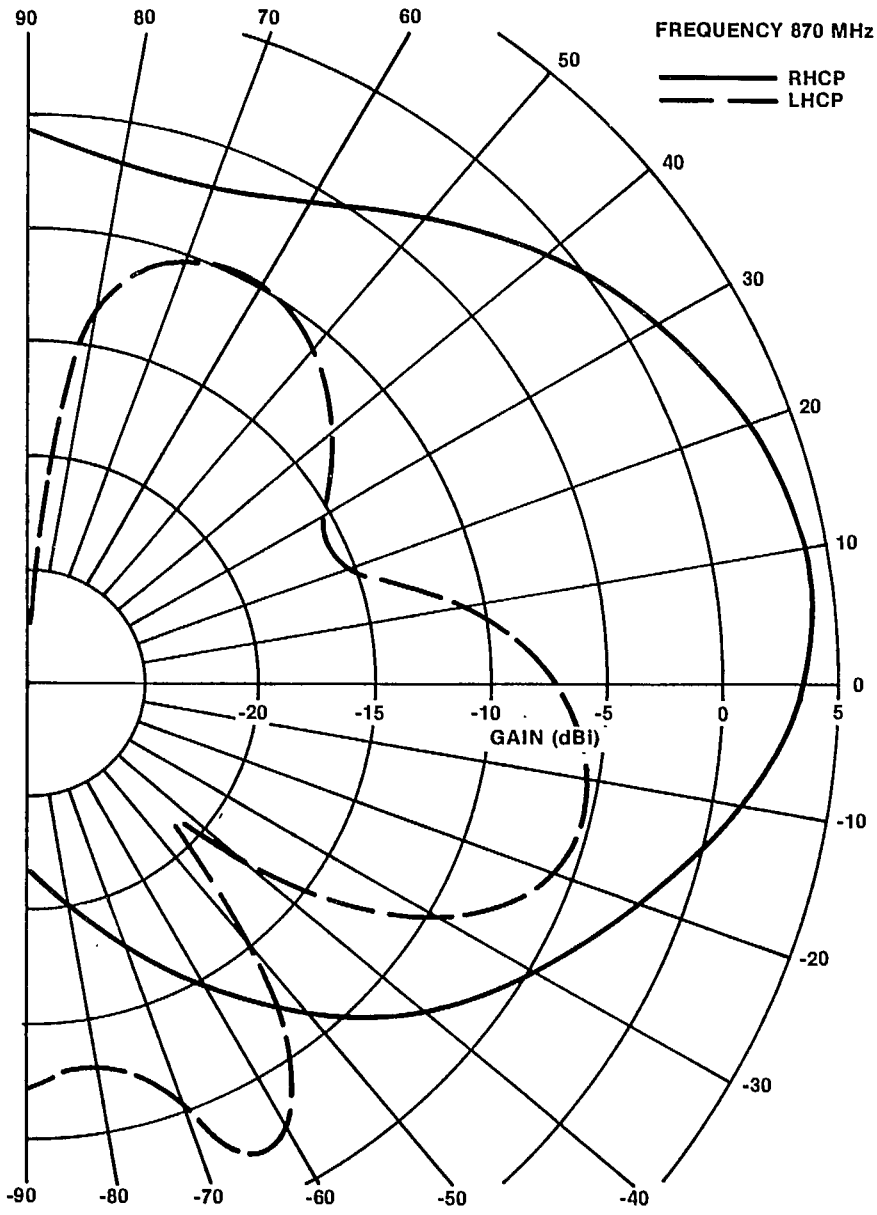

Fig. 14 Elevation-plane pattern of the unmounted conical-log-spiral antenna

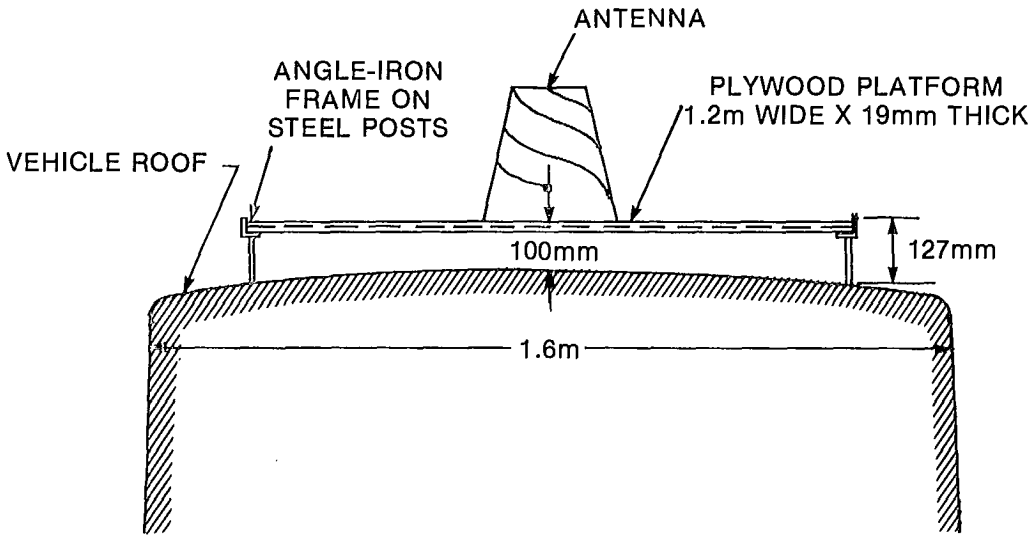

Fig. 15 Details of the antenna mounting on the vehicle roof

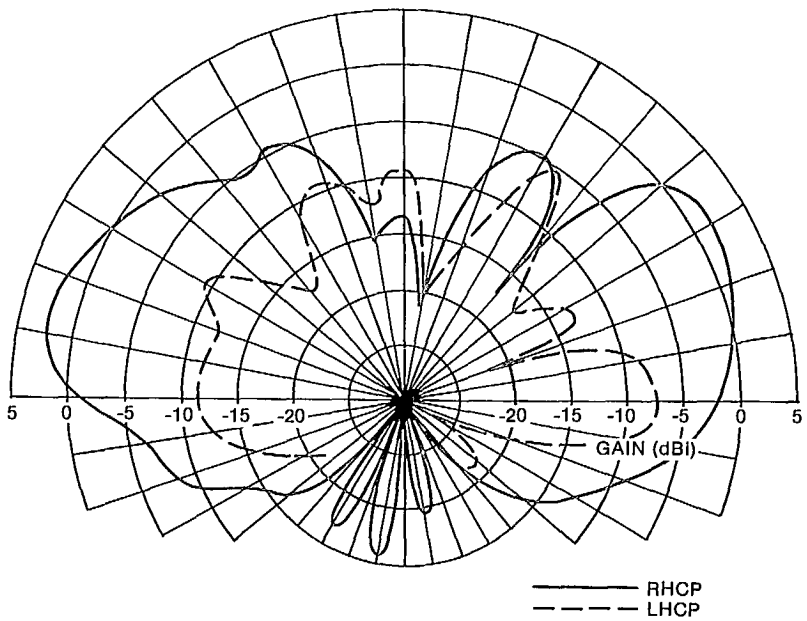

Fig. 16 Broadside antenna elevation-plane pattern as-mounted on the vehicle roof

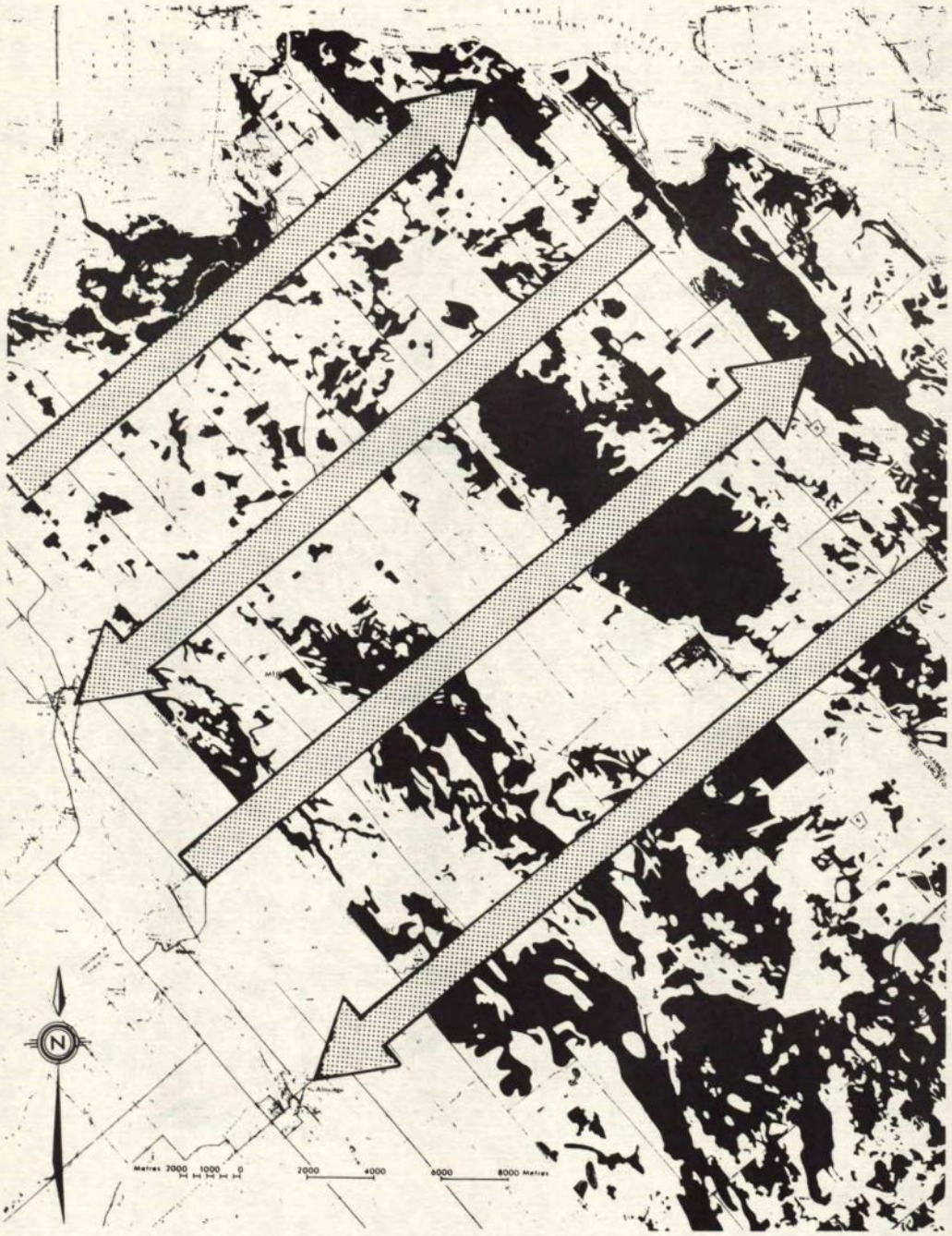

Fig. 17 Map showing the routes followed. Woodlands (shown dark) constitute 35% of the land area

Fig. 18 Helicopter with mounted transmitter/antenna package

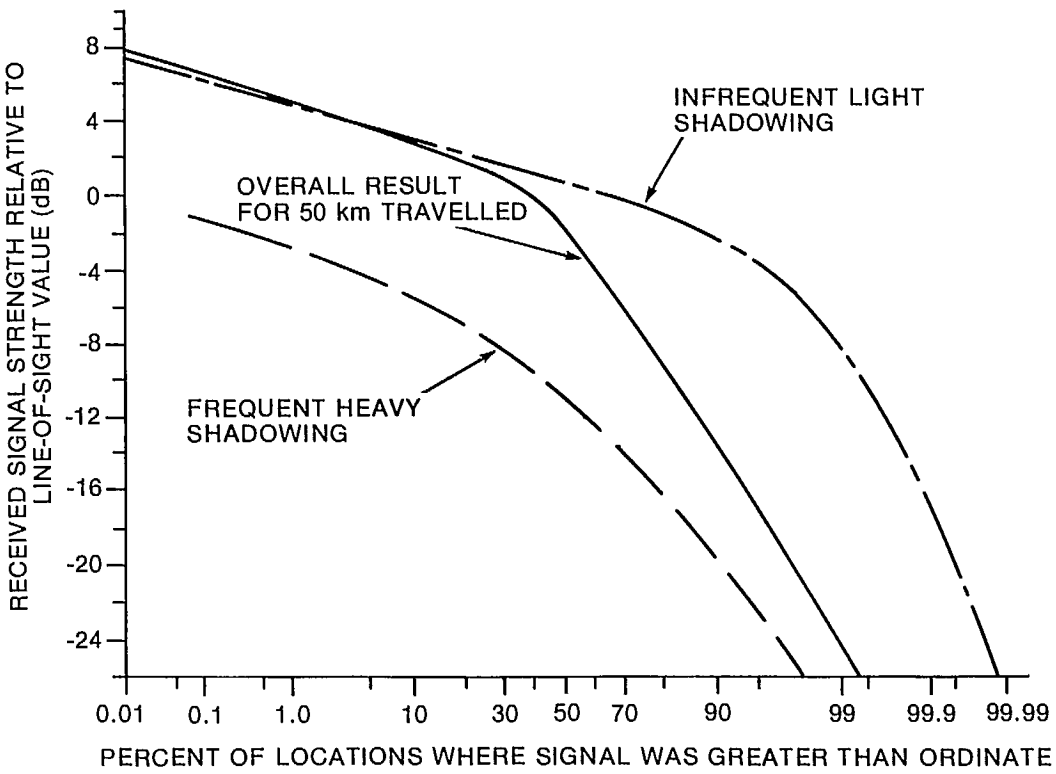

Fig. 19 Cumulative distribution functions for September 1982 data

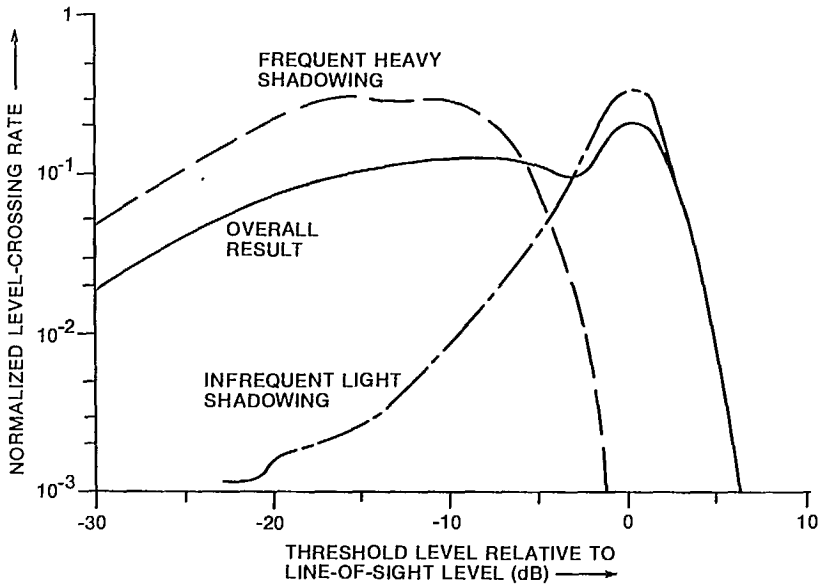

Fig. 20 Normalized level-crossing rate (number of positive crossings per wavelength travelled) for September 1982 data

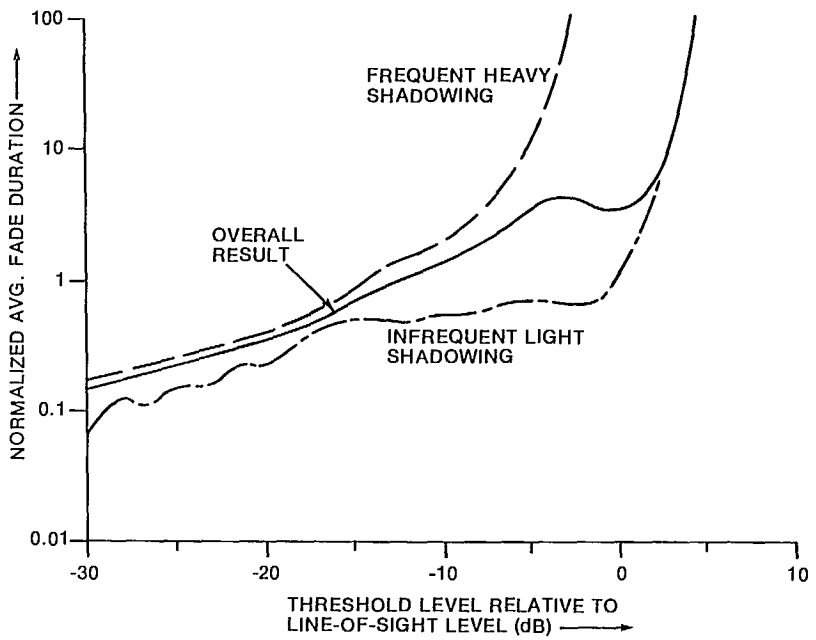

Fig. 21 Normalized average fade duration (in multiples of a wavelength travelled) for September 1982 data

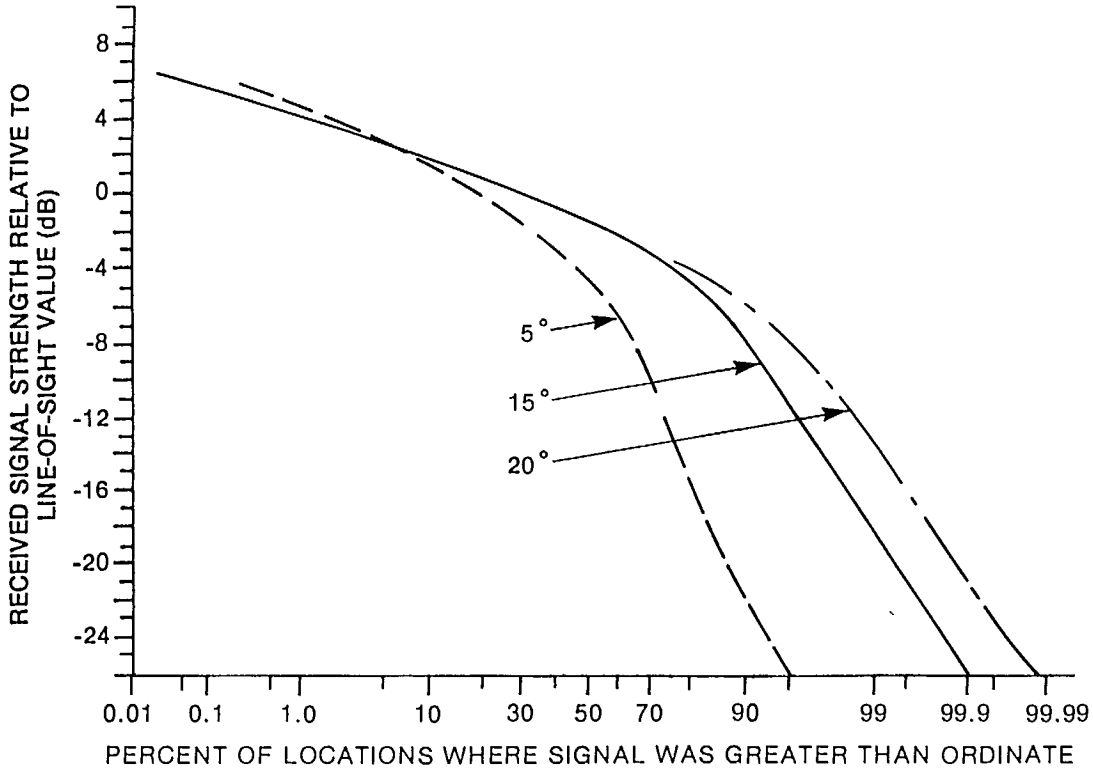

Fig. 22 Distribution functions for June 1983 data

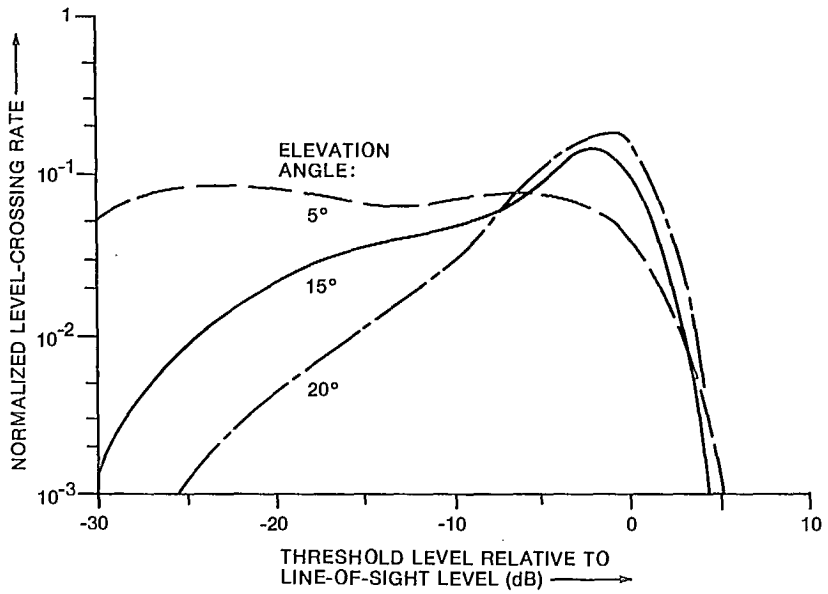

Fig. 23 Normalized level-crossing rate (number of positive crossings per wavelength travelled) for June 1983 data

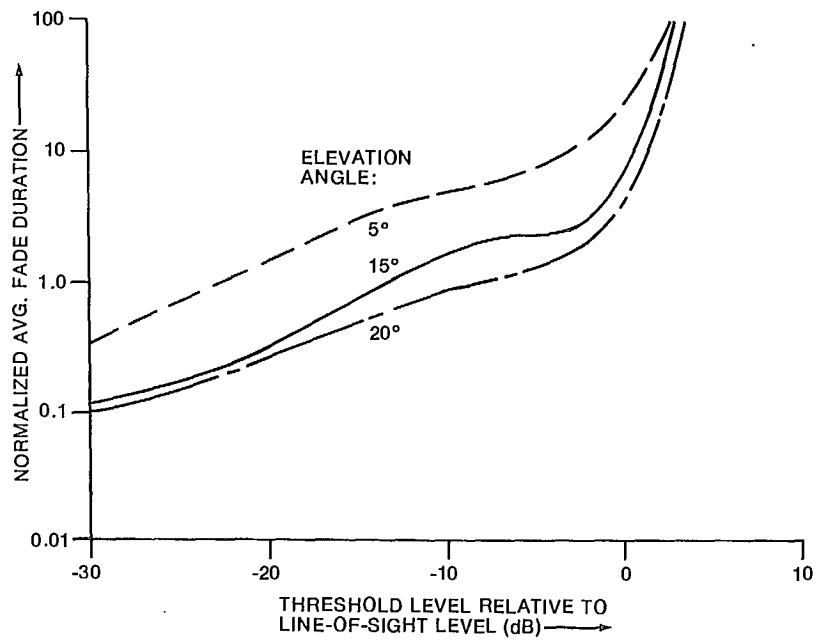

Fig. 24 Normalized average fade duration (in multiples of a wavelength travelled) for June 1983 data

A P P E N D I X A

Description of the Data Acquisition Program

The program HELICO, written in BASIC, is designed to acquire real-time digitized data from the high-speed DVM connected to the receiver video output. Data are transferred from the DVM to the computer via the IEE 488 interface bus (GPIB) for storage on a floppy disc. A GPIB-controllable relay actuator is also used to enable computer control of the instrumentation tape-recorder used for making "stored-channel" recordings.

Figure A1.1 shows a flow-chart of "HELICO". The program starts with the definition of variables, the assignment of input and output addresses for external equipment, a reset to zero for external equipment and a pause permitting the operator to insert an initialized floppy disc. The following steps calibrate the spectrum analyser. Generally, it has been the operator's choice to perform this calibration once only for each test period (usually about 3 hours). The calibration routine is built into the spectrum analyser and takes 1-2 minutes to complete. The necessary calibration factors are retained by the analyser and applied automatically to the measurements.

When the calibration is completed, the program passes to control and verification of the measurement equipment. The state of the spectrum analyser is set to certain default values, namely 871 MHz centre-frequency, 300 Hz resolution bandwidth, 10 KHz video bandwidth and -20 dBm reference level. The file name and the amount of storage space available on the disc are verified next, then the initial information for the impending test is displayed on the computer screen. At the same time several "soft-keys" are defined which permit changes to any of the default values.

There are ten "soft-keys" which provide the operator with a great deal of flexibility in determining the flow of the program. Briefly, these functions are:

Key 0. RETURN/CONTINUE: permits a return to the analyser calibration, if desired.

Key 1. LINE-OF-SIGHT = YES/NO?: when pressed, this key permits the taking a data sample of 1000 points under unshadowed conditions.

Key 2. N-SAMPLE: permits specification of the sample size for the test. Each sample uses two bytes of storage capacity. The discs have a total capacity of 260 k bytes. It is also possible to specify sample size in terms of distance travelled, in which case the maximum distance is 6.5 km.

Key 3. ON/OFF_T: permits the operator to enable or disable operation of the instrumentation tape-recorder.

Key 4. S/N : permits evaluation of the received signal-to-noise power density ratio. Moves marker to read peak signal power, then moves marker off signal to read noise power.

Key 5. FI NAME: this key can be used to set the file name.

Key 6. SETDATE: permits entry of experiment date.

Key 7. SETTIME: permits entry of standard time (UTC).

Key 8. CEN.FREQ: permits entry of spectrum analyser centre frequency, with a default value of 871 MHz.

Key 9. BANDWIDTH: permits selection of spectrum analyser resolution bandwidth from the discrete values of 30,100, 300 and 1000 Hz, with a default value of 300 Hz.

Having selected "CONTINUE" with Key 0, the program prepares the measurement system for taking data. This consists of creating a data file to receive the sample points and of setting the equipment into the correct mode of operation. This setting includes the programming of the digital voltmeter (1 volt scale, external or internal clock, etc.) and, of particular importance, the tuning of the spectrum analyser to the precise frequency of the source signal. The video output of the spectrum analyser varies between 0 and 1.5 volts, where 1 volt corresponds to the chosen "reference level" of the analyser. The reference level is determined automatically by the program to be twice the amplitude of the mean signal level under line-of-sight conditions. The analyser is used in linear mode rather than logarithmic, because of the requirement to record the quadrature-demodulated IF output for "stored-channel" use.

Signal sampling starts by reading the selected analyser reference level, starting the instrumentation tape-recorder and reserving memory space for the data points. The maximum size of each file is 130,000 points, which calls for 260 k bytes of active memory. The data acquisition rate may vary up to a maximum of 1000 samples/second. When the desired number of data points have been acquired, the computer structures the file and transfers the data to disc. When the transfer is completed, the program gives access to three "soft-keys" called "STOP PRG", "NEW FILE" and "ON/OFF_T". These keys enable the operator to start a new test, terminate the session or to turn the tape-recorder on or off.

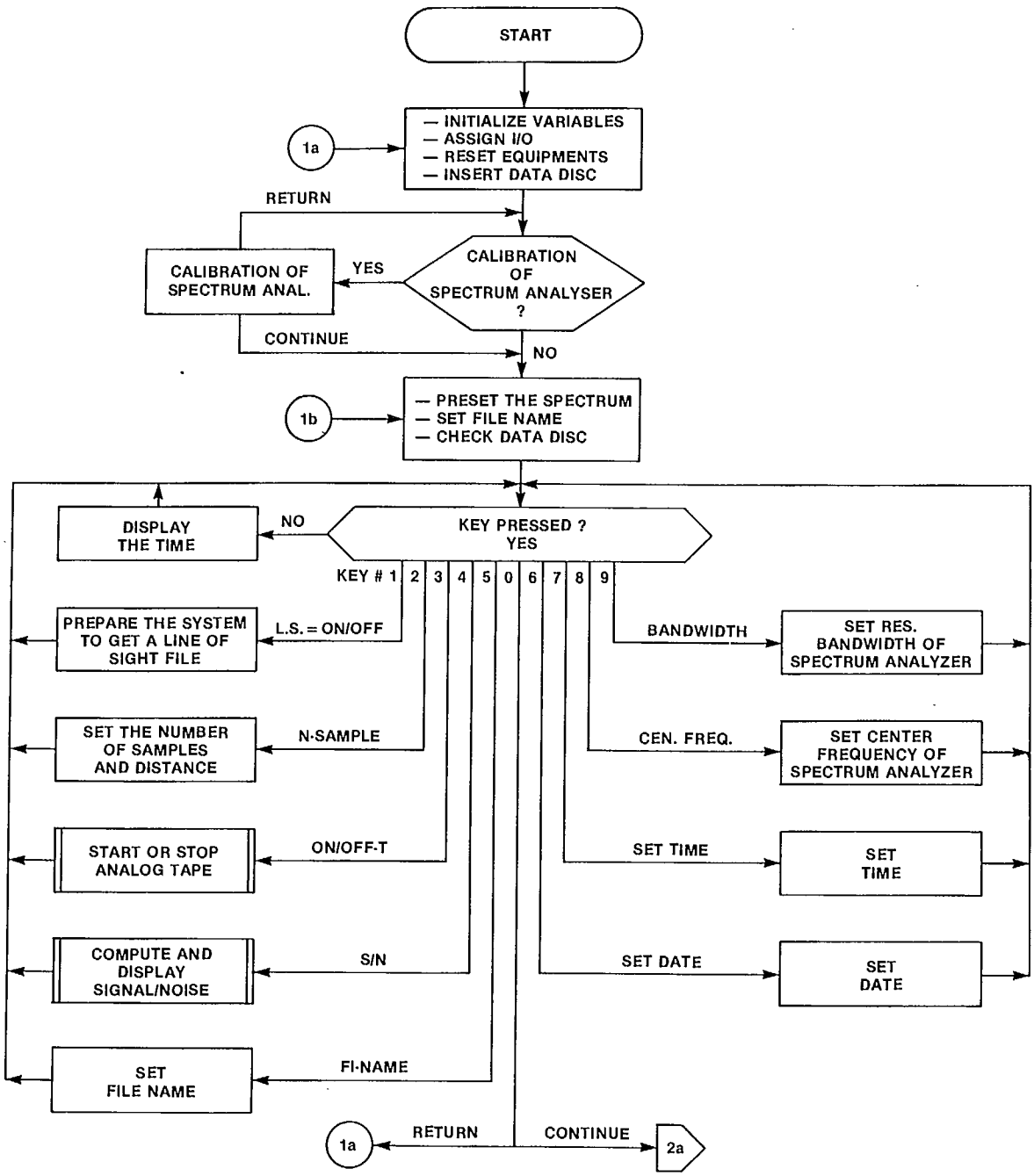

Fig. A1.1 Flow-Chart for "HELICO"
(continued on next page)

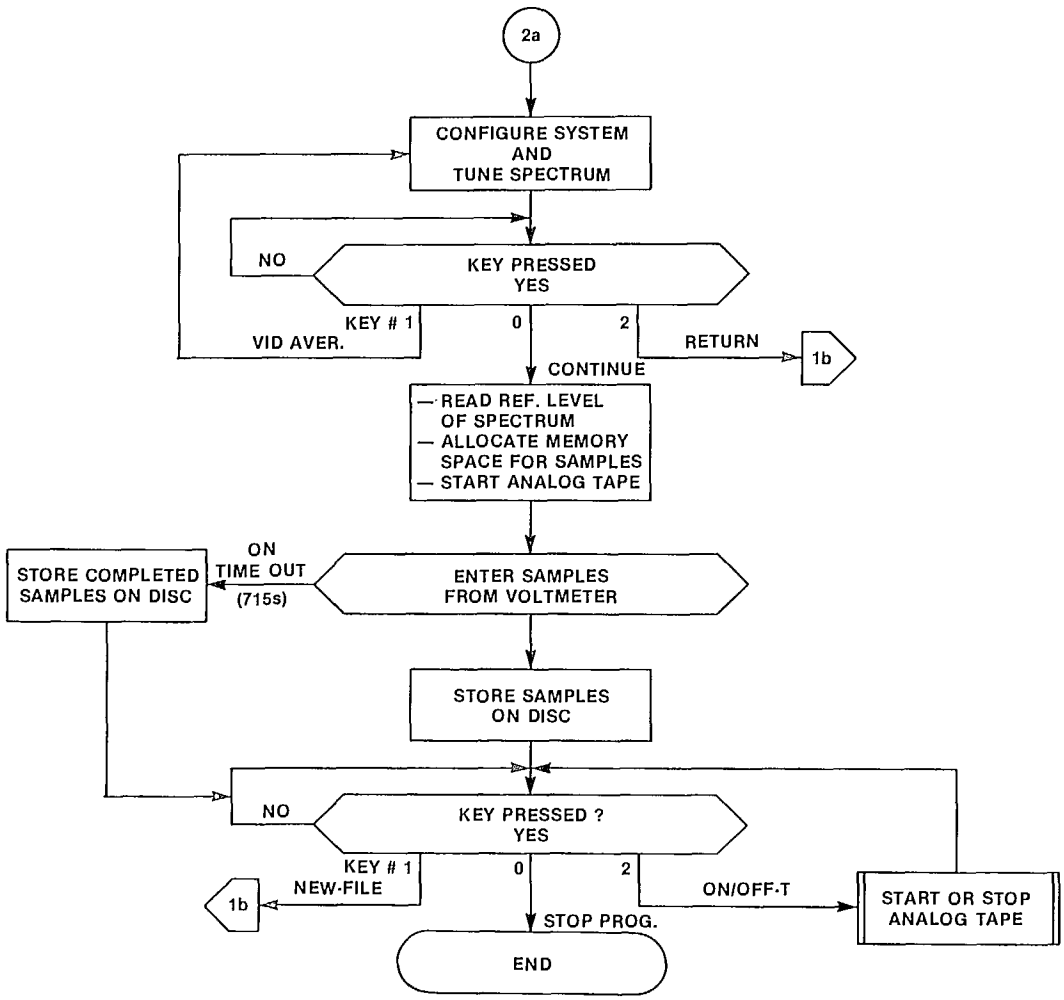

Fig. A1.1 (continued)

A P P E N D I X B

Description of the Data Analysis Program

Figure A2.1 shows a flow-chart of the program "HELPLOT". The program begins by a definition of variables and verification of the presence or absence of an external printer. In the absence of a printer, results are shown only on the internal CRT display. Pertinent information such as a list of file names on the disc in use is shown on the screen at the same time as the definition of a number of "soft-keys" which give the operator control over the flow of the program. The functions of these eight keys are:

Key 0. CONTINUE: used to start the analysis

Key 1. L SIGHT: used to calculate the median value of a signal sample taken in an unshadowed area

Key 2. SET NAME: allows operator to set file name

Key 3. PRINT: displays information on the screen

Key 4. DUMP: prints the analysis results on the external printer

Key 7. SUM: data analysis is performed file-by-file. The results are accumulated for all files when the "SUM" key is activated. Accumulation is performed after analysis of each file and the cumulated totals are stored in a file called "SUM" which includes the following data:
- median level of line-of-sight signal sample (V_R)
- total number of data points
- distribution of cumulated signal amplitudes ($P_{xt}(X)$) (grouped into class intervals of 1 dB)
- distribution of cumulated normalized level-crossing rate ($LCR_{n,xt}(X)$) (grouped into class intervals of 1 dB).

Key 8. CLR SUM: resets to zero the active memory registers containing the cumulated totals.

Key 9. RCL SUM: recalls cumulated totals, etc. into the active memory registers.

When the appropriate operating conditions have been selected with the aid of these keys, the analysis is started. The data is read and the amplitude distribution of the signal sample, $P_x(X)$, the normalized level-crossing rate, $LCR_n(X)$, and the normalized average fade duration, $FD_n(X)$, are calculated. The amplitude distribution of the signal is calculated on a logarithmic (dB) scale. The scale range extends from -45 to +10 dB, where 0 dB corresponds to the median level of the signal sample taken under unshadowed conditions. The scale is divided into 56 class intervals with centres corresponding to the integers +10, +9,

....-44, -45. The 54 central classes are consequently of width 1 dB and the two extreme classes are "open" at their extreme ends. The decoded amplitude data are thus stored as vectors which are cumulated for each of the 56 class intervals.

At the same time, the program calculates the level-crossing rate for the various signal levels. To do this, each sample point is compared with its predecessor. When the difference in level is found to increase from the predecessor to the sample point under consideration, a positive level crossing has occurred for each of the class intervals between the levels of the two data points. The vectors representing each of these class intervals are then incremented by one. At the end of the analysis one thus obtains a set of vectors (one for each class interval) giving the number of positive crossings, $P_+(X)$. From this, the normalized level-crossing rate is calculated:

$$LCR_n(X) = \frac{P_+(X)}{Nd}$$

= signal source wavelength
N = number of data points in the sample
d = distance between data points (5 cm)

The normalized average fade duration can be obtained directly from the two preceding functions, $P_x(X)$ and $LCR_n(X)$. It is calculated from the relationship*:

$$FD_n(X) = \frac{F_x(X)}{LCR_n(X)} \quad -45 \leqslant X \leqslant 10 \text{ dB}$$

Here $F_x(X)$ is the cumulative distribution function of the data, calculated by numerical integration of the density function $P_x(X)$. To perform this integration, the centre-points of the top of each bar of the relative frequency histogram are conceptually joined to form a frequency polygon. The distribution function is then obtained by numerical integration of the frequency polygon using the trapezoidal rule.

The cumulation of results from several files is relatively simple. As an example, consider two files f_1 and f_2 with statistics $P_{x1}(X)$, $P_{x2}(X)$, $LCR_{n\ x1}(X)$, $LCR_{n\ x2}(X)$, from which it is desired to calculate the statistics of a third file, f_t, formed from the union of f_1 and f_2. As already discussed, for the amplitude distribution it is only necessary to cumulate the vectors for each class-interval. For the level-crossing rate, a weighted mean must be calculated. From the definitions:

---

*Lee, W.C.Y., 1982, "Mobile Communications Engineering", New York, McGraw-Hill, Section 2.8

$$LCR_{n\ x1}(X) = \frac{\lambda}{d} \frac{P_{+\ x1}(X)}{N_1}$$

$$LCR_{n\ x2}(X) = \frac{\lambda}{d} \frac{P_{+2\ x2}(X)}{N_2}$$

it follows that:

$$LCR_{n\ xt}(X) = \frac{\lambda}{d} \frac{P_{+,x1}(X) + P_{+\ x2}(X)}{N_1 + N_2}$$

By re-arrangement of terms, the following expression is obtained:

$$LCR_{n\ xt}(X) = \frac{N_1\ LCR_{n\ x1}(X) + N_2\ \ LCR_{n\ x2}(X)}{N_1 + N_2}$$

This last equation (extended to an indeterminate number of files) is used to obtain the level-crossing rate for the concatenated data.

Finally, the average fade duration for the union of several files is obtained from:

$$FD_{n\ xt}(X) = \frac{F_{xt}(X)}{LCR_{n,xt}(X)}$$

Having completed the analysis and displayed the results, the program returns control to the operator. By the use of"soft-keys" the operator can choose to end the program or continue with the analysis of new data.

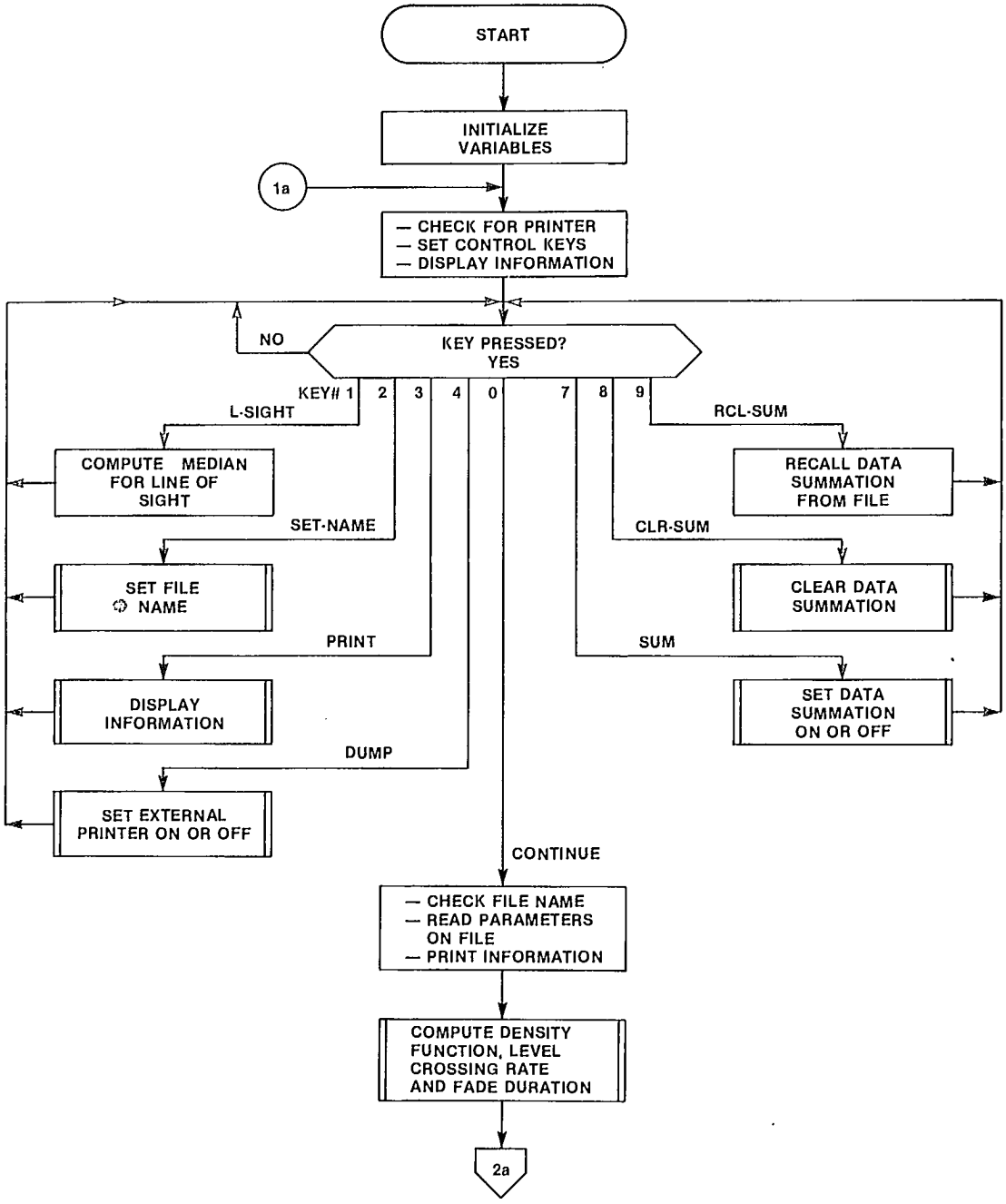

Fig. A2.1 Flow-Chart for "HELPLOT"
(continued on next page)

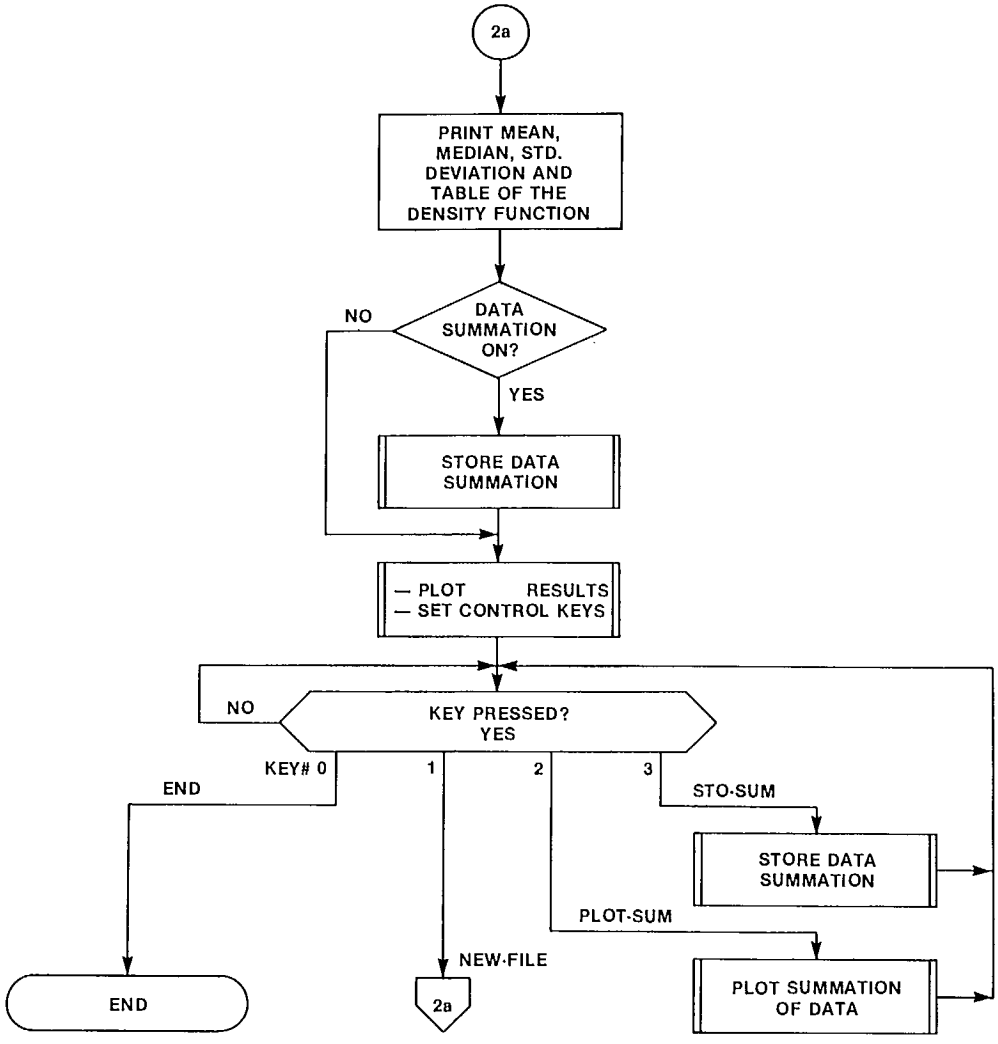

Fig. A2.1 (continued)

APPENDIX C

Specular Reflection at Low Elevation Angles

A3.1 INTRODUCTION

At higher satellite elevation angles, the specularly reflected wave (energy coherently reflected from the ground in the satellite direction) arrives at the mobile antenna from a depression angle equal to the satellite elevation angle. Consequently it is usually in the back or side-lobe region of the antenna and so is received at a much-reduced level. Above the Brewster angle (15° for land mobile) the reflected signal is also reversed in polarization compared to the direct signal and so, depending on mobile antenna characteristics, may be reduced through polarization coupling loss.

At elevation angles below the Brewster angle, the polarization sense is not reversed and, particularly below 10° elevation angle, the antenna directivity does not usually provide much attenuation for the reflected wave. This is one reason why specular reflection is usually only significant at low source elevation angles.

A second reason is that the reflected wave from a rough surface, unlike that from a smooth surface, reduces in amplitude with increasing elevation angle, once again providing for worst conditions at low angles. Experimental measurements made with an omni-azimuth mobile antenna at 5° elevation angle have indicated the likely presence of a strong specular component. Fade depths of 7 - 8 dB were observed with a period of several seconds, clearly distinguishing this type of fading from diffuse multipath fading which has a lower range and a very short period. No evidence of specular reflection was observed at 15° or higher elevation angles.

This appendix will summarize the theoretical aspects of specular reflection and will provide predictions of the reflected signal strength, fade depth and fading rate under various assumptions.

A3.2 CALCULATION OF SPECULAR REFLECTION COEFFICIENT

The specular reflection coefficient for a curved, rough surface is usually calculated using the following expression (Beckmann, 1963, p. 244):

$$R_S = \rho_S \, D R_0$$

where:

ρ_S = the surface roughness factor
D = curved earth divergence factor
R_0 = complex voltage reflection coefficient for smooth, plane earth

A3.2.1 SURFACE ROUGHNESS FACTOR

This is one of the more difficult factors to estimate and generally requires empirical data for accuracy. The surface roughness factor depends on the standard deviation of irregularity heights, σ_i and the grazing angle, α, in the following way (Beckmann, 1963, p. 316):

$$\rho_S = \exp -1/2 \left[4\pi \, (\mathrm{Sin}\ \alpha) \, \sigma_i/\lambda\right]$$

As an example, the dependence of surface roughness on grazing angle is plotted in Figure A3.1 for σ_i = 0.1 m and 870 MHz (σ_i/λ = 0.3). For this example, the earth is considered "smooth" below a grazing angle of nine degrees, according to the Rayleigh Criterion:

$$h < \lambda/(8 \ \mathrm{Sin}\ \alpha)$$

Taking h as the 10% to 90% irregularity height, then σ_i = h/2.56 and for the surface to be considered smooth we need to have:

$$\sigma_i < 1/(20.5 \ \mathrm{Sin}\ \alpha)$$

i.e. $\alpha < 9^\circ$ for h = 0.26 m at 870 MHz.

It is probable that the flat grassland parts of the test area, over which long-period fading effects were observed, meet the Rayleigh Criterion as stated above, and so the surface roughness factor is essentially equal to unity for elevation angles below nine degrees.

A3.2.2 DIVERGENCE FACTOR

The divergence factor is a measure of the spreading of the reflected energy due to the earth's curvature. It is of importance where the mobile terminal is at an appreciable height above the earth, e.g. an aircraft terminal. For land-mobile applications, its value is unity for all practical elevation angles, as shown in Fig. A3.2, where the parameter h is the height of the mobile antenna.

A3.2.3 PLANE-EARTH REFLECTION COEFFICIENT

The usual practice is to calculate the plane-earth reflection coefficient from measured values of soil conductivity and relative permeability. These factors depend strongly on soil moisture content. The values proposed in CCIR Recommendation 527-1 for medium-dry soils will be used here. These lead to the values of reflection coefficient shown in Fig. A3.3 (Hall, 1979, p. 88).

The horizontally-polarized component is always phase-shifted by 180° on reflection. The vertical component is not phase-shifted at angles above the Brewster angle; below the Brewster angle it is shifted by 180°. For incident RHCP, the major reflected component above the Brewster

angle is LHCP with varying axial ratio. Below the Brewster angle it is RHCP with varying AR.

A3.2.4 CALCULATION OF REFLECTED COMPONENT LEVELS

Taking the value of 0.1 m assumed previously for σ_i, one can calculate the relative amplitude of the reflected wave using the information in Fig. A3.1, A3.2 and A3.3. This is shown in Fig. A3.4, where the right and left-hand circularly-polarized components have been calculated from:

$$(RHCP)_S = \rho_S(\rho_H + \rho_V)/2$$

$$(LHCP)_S = \rho_S(\rho_H - \rho_V)/2$$

Here ρ_V is a complex number which changes from positive below the Brewster angle to negative above the Brewster angle. At all values of grazing angle, the major axis of the polarization ellipse is horizontal.

A3.3 FADE DEPTHS WITH THE CONICAL LOG-SPIRAL ANTENNA

In order to calculate the fade depth, the effects of the antenna gain patterns for RHCP and LHCP must be superimposed on the reflected wave. For the omni-azimuth vehicle antenna used for experimental measurements the elevation-plane pattern was shown previously in Fig. 14. The fade depth is calculated from:

$$FD = 20 \log \frac{G_D - G_R\,(RHCP)_S}{G_D}$$

An assumption is that the received LHCP wave, $G_R(LHCP)_S$, is negligible. This should certainly be the case. The results obtained are shown in Fig. A3.5, again using $\sigma_i = 0.1$ m. One can see that maximum fade depths climb rapidly below ten degrees elevation.

A3.4 FADING RATES FOR SPECULAR REFLECTIONS

Taking a source elevation angle of five degrees as an example, the mobile will need to move about 30 m towards or away from the source in order to pass through one fading cycle, i.e. from addition of direct and reflected wave, through subtraction and back to addition. With diffuse multipath reflections, where the mobile is moving through a standing-wave field of multiple reflections, the corresponding distance is a half-wavelength or 0.17 m. Fading due to specular reflection at five degrees can therefore be distinguished because it occurs at a rate about two hundred times slower than that due to diffuse multipath.

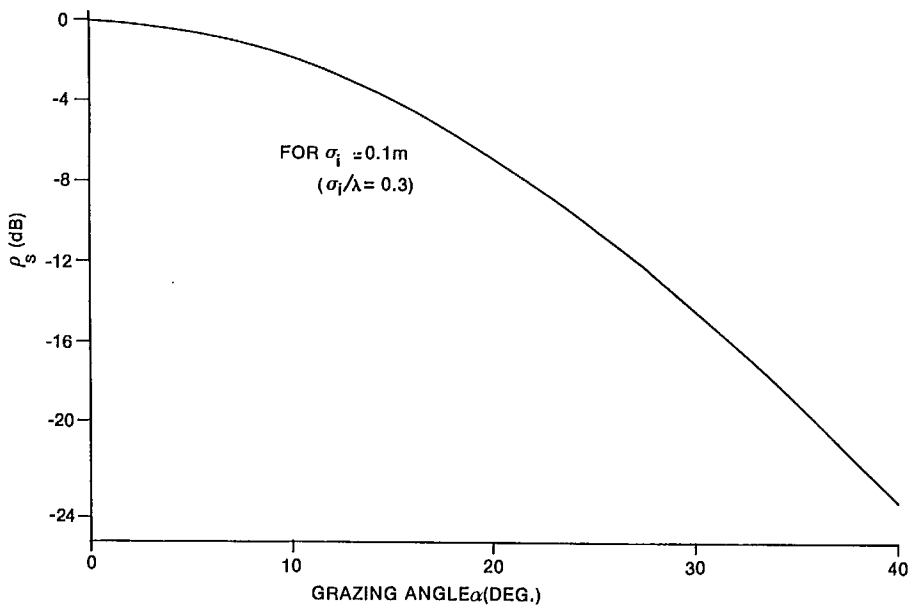

Fig. A3.1 Variation of surface roughness factor with grazing angle

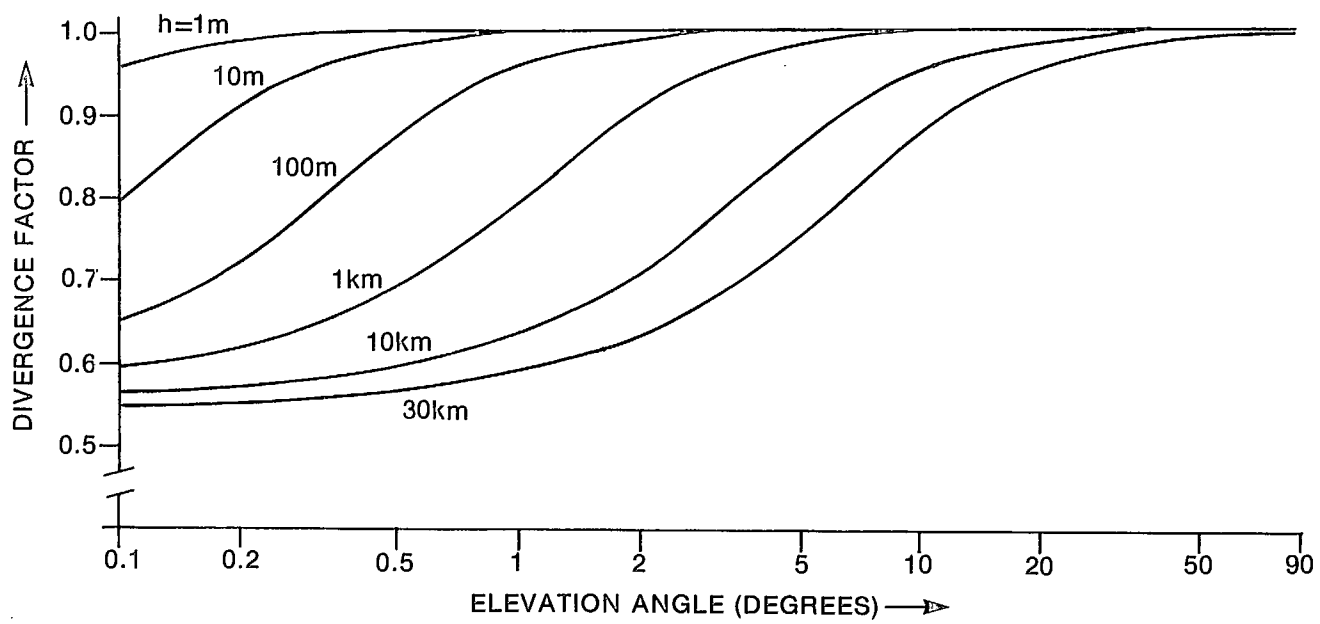

Fig. A3.2 Divergence factor for the geostationary satellite-to-mobile terminal case. Parameter h is the mobile antenna height above the earth's surface

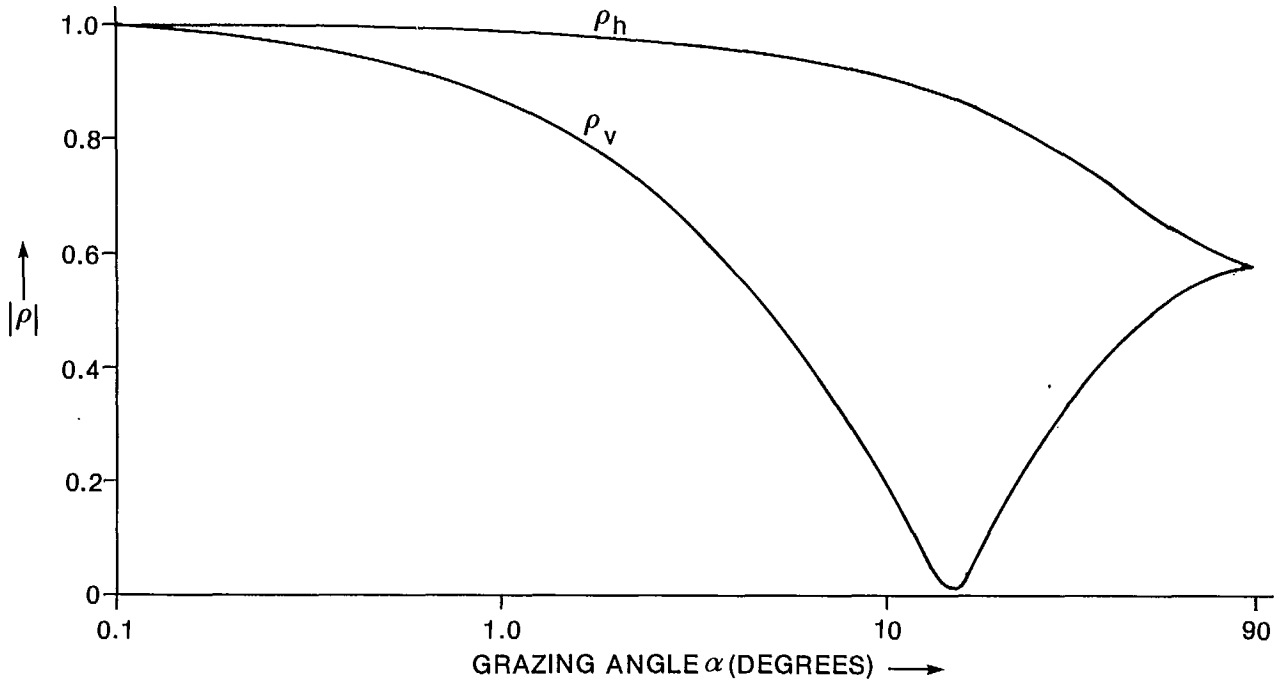

Fig. A3.3 Reflection coefficients of medium-dry ground as a function of grazing angle

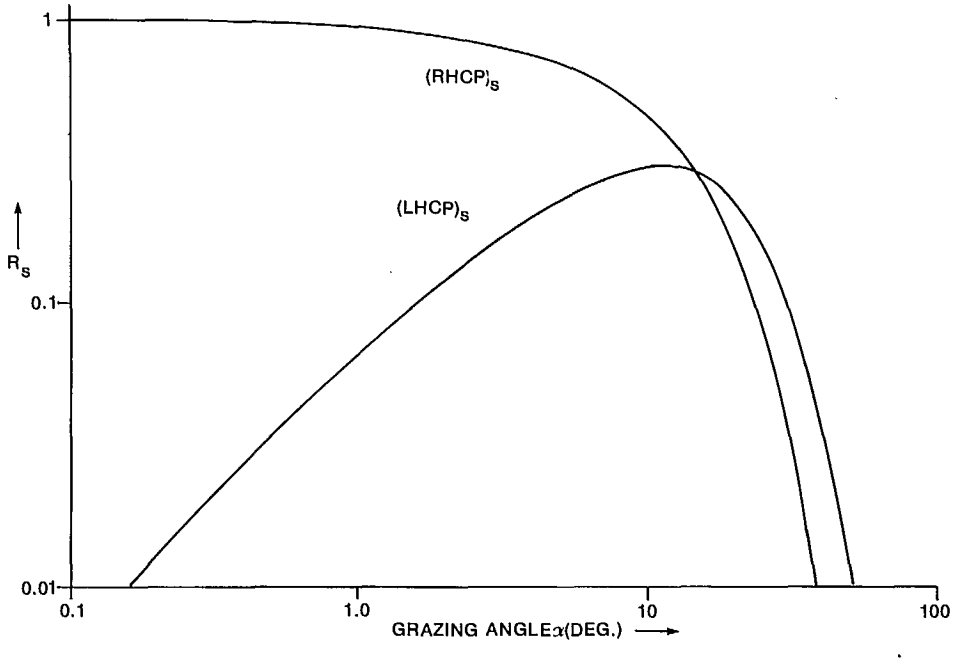

Fig. A3.4 Components of the specular reflection coefficient as a function of grazing angle

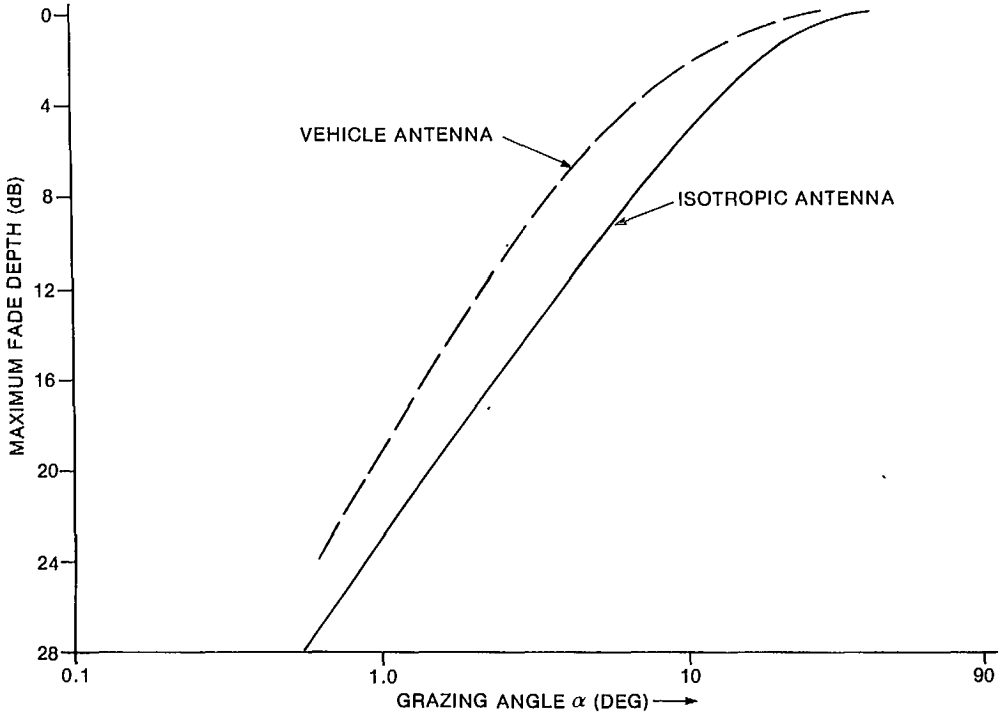

Fig. A3.5 Variation of maximum fade depth with grazing angle